GENE EXPRESSION IN *LUCILIA SERICATA* (DIPTERA: CALLIPHORIDAE) LARVAE EXPOSED TO *PSEUDOMONAS AERUGINOSA* AND *ACINETOBACTER BAUMANNII*

A Thesis

by

CLAIRE HELEN MCKENNA

Submitted to the Office of Graduate and Professional Studies of
Texas A&M University
in partial fulfillment of the requirements for the degree of

MASTER OF SCIENCE

Chair of Committee,	Jeffery K. Tomberlin
Committee Members,	Aaron M. Tarone
	Tawni Crippen
Head of Department,	David W. Ragsdale

May 2017

Major Subject: Entomology

ABSTRACT

The green bottle fly (*Lucilia* sericata) larvae are amongst the first colonizers of carrion and are well studied for their impact in forensics, decomposition ecology, and medicine. The larvae of *L. sericata* are the only FDA approved species for maggot therapy and can be successful in wound debridement, disinfection, and contribute to wound healing and tissue regeneration. Because these larvae naturally colonize habitats with high microbial loads, it is not surprising that they have a large repertoire of antimicrobial peptides. In this study, 2nd instar *L. sericata* larvae were exposed to Gram-negative bacteria (*Pseudomonas aeruginosa* or *Acinetobacter baumannii*) and evaluated for differences in transcript abundance due to bacterial exposure identified through RNA-seq analysis. Differentially expressed genes were identified and characterized by analyzing RNA-seq data with traditional software analysis and gene ontology methodologies. Up-regulated and down-regulated genes included those associated with the recognition, signaling cascades, and effector molecule transcription of the insect immune response pathways. Differentially expressed transcripts also included some previously identified antimicrobial peptides. Other differentially expressed genes were uncharacterized and so functions were not attributed to these genes. The data produced in this study may contribute to future studies such as the potential identification of new antimicrobial peptides, genome editing or genetic engineering of Medical Maggots™, and transcriptome studies in *L. sericata* as well as other organisms.

ACKNOWLEDGEMENTS

I would like to thank my committee chair, Dr. Tomberlin, and my committee members, Dr. Tarone, and Dr. Crippen, for their guidance and support throughout the course of this research.

Thanks also go to my former and current colleagues and the department faculty and staff for making my time at Texas A&M University a great experience. I also want to extend my gratitude to the staff at the USDA for their help in conducting experiments.

Finally, thanks to my family and friends for their encouragement and to my son Connor, who was born during this project and so has been involved with it for his whole life.

CONTRIBUTORS AND FUNDING SOURCES

This work was supervised by a thesis committee consisting of Dr. Jeffery Tomberlin (Advisory chair) and Dr. Aaron Tarone of the Department of Entomology and Dr. Tawni Crippen of the USDA.

All work for the thesis was completed independently by the student.

Graduate study was supported by Texas AgriLife Research Genomics Seed Grant Program 2014. The focus of this portion of the grant was titled "Characterizing the functional dynamics between microbial wound communities and the biodebridement species, *Lucilia sericata*, to improve wound healing."

NOMENCLATURE

h	hour(s)
min	minute(s)
CFU	Colony Forming Units
PMI	Postmortem Interval
MDT	Maggot Debridement Therapy
TSA	Trypticase Soy Agar
PBS	Phosphate Buffered Saline
VOCs	Volatile Organic Compounds
GO	Gene Ontology

TABLE OF CONTENTS

Page

ABSTRACT ii

ACKNOWLEDGEMENTS iii

CONTRIBUTORS AND FUNDING SOURCES iv

NOMENCLATURE v

LIST OF FIGURES vii

LIST OF TABLES x

CHAPTER I INTRODUCTION AND LITERATURE REVIEW 1

- Interactions Between Microbes and Insects 2
- Metagenomic Analysis 3
- Medical and Economic Threat of Drug Resistant Pathogens 4
- Maggot Debridement Therapy and Success of *L. sericata* 6
- Objectives and Hypothesis 8

CHAPTER II RESEARCH, RESULTS, AND DISCUSSION 10

- Introduction 10
- Materials and Methods 12
- Results 20
- Discussion 67

CHAPTER III FUTURE STUDIES AND LIMITATIONS 71

REFERENCES 73

LIST OF FIGURES

Page

Fig. 1: Larvae just below surface of agar in 5 mL round bottom tube. 20

Fig. 2: Example summary of TopHat alignment output with default parameters. 22

Fig. 3: Heatmap displaying relative expression levels of genes that are differentially expressed between larvae exposed to *P. aeuruginosa* for one hour (PA1) and control group larvae (C1). Expression levels between samples are compared in terms of log10 normalized mapped read (FPKM) values. Light beige coloring corresponds to lower levels of gene expression and dark orange coloring corresponds to higher levels of gene expression..... 26

Fig. 4: Scatterplot of pairwise gene expression levels between AB4 and C4 with log10 transformed fpkm values. Genes that are differentially expressed at a significant level are highlighted and labeled. A data point above y=x represents a gene that is expressed at higher level in AB4 than in C4..... 33

Fig. 5: Scatterplot of pairwise gene expression levels between PA4 and C4 with log10 transformed fpkm values. Genes that are differentially expressed at a significant level are highlighted and labeled. A data point above y=x represents a gene that is expressed at higher level in PA4 than in C4. 34

Fig. 6: Four-way Venn diagram displaying overlapping counts of significant differentially expressed genes that are down-regulated. 36

Fig. 7: Four-way Venn diagram displaying overlapping counts of significant differentially expressed genes that are up-regulated. 37

Fig. 8: Barplot displaying expression level fpkm values for gene FF38_01452 (AB4 vs C4). Gene FF38_01452 is associated with a peptidoglycan catabolic process (the chemical reactions and pathways resulting in the breakdown of peptidoglycans, any of a class of glycoconjugates found in bacterial cell walls). FF38_01452 is also up-regulated in PA4 vs C4. 38

Fig. 9: Example summary of TopHat alignment output with increased mismatch rate and read edit distance parameters..... 39

Fig. 10: Heatmap displaying relative expression levels of genes that are differentially expressed between larvae exposed to *A. baumannii* for one hour (AB1) and control group larvae (C1). 45

Fig. 11: Scatterplot of pairwise gene expression levels between AB1 and C1 with log10 transformed FPKM values. Genes that are differentially expressed at a significant level are highlighted and labeled. A data point above y=x represents a gene that is expressed at higher level in AB1 than in C1. 46

Fig. 12: Scatterplot of pairwise gene expression levels between PA1 and C1 with log10 transformed FPKM values. Genes that are differentially expressed at a significant level are highlighted and labeled. A data point above y=x represents a gene that is expressed at higher level in PA1 than in C1. 47

Fig. 13: Scatterplot of pairwise gene expression levels between AB4 and C4 with log10 transformed FPKM values. Genes that are differentially expressed at a significant level are colored pink. A data point above y=x represents a gene that is expressed at higher level in AB4 than in C4. 57

Fig. 14: Scatterplot of pairwise gene expression levels between PA4 and C4 with log10 transformed FPKM values. Genes that are differentially expressed at a significant level are highlighted and labeled. A data point above y=x represents a gene that is expressed at higher level in PA4 than in C4. 58

Fig. 15: Four-way Venn diagram displaying overlapping counts of significant differentially expressed genes that are down-regulated. 60

Fig. 16: Four-way Venn diagram displaying overlapping counts of significant differentially expressed genes that are up-regulated. 62

Fig. 17: Barplot displaying expression level fpkm values for gene FF38_01452 (AB4 vs C4). Gene FF38_01452 is associated with a peptidoglycan catabolic process (the chemical reactions and pathways resulting in the breakdown of peptidoglycans, any of a class of glycoconjugates found in bacterial cell walls). FF38_01452 is also up-regulated in PA4 vs C4. 63

Fig. 18: Panther GO-Slim Biological Process pie chart displaying biological process categories for up-regulated genes from the AB4 vs C4 dataset. Gene ontology analysis was performed only for genes that had orthologous genes in *D. melanogaster* that could be mapped to a Panther GO-slim biological process. 65

Fig. 19: Panther GO-slim molecular function bar chart displaying molecular function categories for up-regulated genes from the AB4 vs C4 dataset. Gene ontology analysis was performed only for genes that had orthologous genes in *D. melanogaster* that could be mapped to a Panther GO-slim molecular function. 66

Fig. 20: TopHat output summary of RNAseq alignment to the *L. sericata* reference genome with default parameters. 67

LIST OF TABLES

Page

Table 1 List of Sample Names 14

Table 2 Summary of Cuffdiff Output with Default TopHat Parameters (AB1 vs C1) 24

Table 3 Summary Table of Cuffdiff Output with Default TopHat Parameters (PA1 vs C1) 25

Table 4 Summary Table of Cuffdiff Output with Default TopHat Parameters (AB4 vs C4) 28

Table 5 Summary Table of Cuffdiff Output with Default TopHat Parameters (PA4 vs C4) 31

Table 6 Summary Table of Cuffdiff Output with Adjusted TopHat Parameters (AB1 vs C1) 41

Table 7 Summary Table of Cuffdiff Output with Adjusted TopHat Parameters (PA1 vs C1) 43

Table 8 Summary Table of Cuffdiff Output with Adjusted TopHat Parameters (AB4 vs C4) 49

Table 9 Summary Table of Cuffdiff Output with Adjusted TopHat Parameters (PA4 vs C4) 54

CHAPTER I

INTRODUCTION AND LITERATURE REVIEW

As a high-energy source, carrion provides essential resources to a large variety of species including plants, insects, vertebrates, and microbes (Parmenter and MacMahon 2009, Barton et al. 2013). In some instances, successional patterns in the presence of these organisms during the decomposition of carrion allows for the determination of forensically relevant information such as the postmortem interval (PMI) and can provide insight about factors surrounding the death and subsequent treatment of the remains (Anderson and VanLaerhoven 1996, Anderson et al. 2000, Boehme et al. 2014). Examination of the types of insect species present and even differences in geographic populations of the same insect species can help determine if remains have been moved from the original site of death to another location (Byrne et al. 1995, Anderson et al. 2000).

Blow flies, such as *Lucilia sericata* (Meigen) (Diptera: Calliphoridae), are amongst the first arthropods to colonize remains (Anderson et al. 2000). They locate remains via attraction to the volatile organic compounds (VOCs) produced by decomposing remains and bacteria (Anderson et al. 2000, Frederickx et al. 2012). The decomposition process produces a variety of VOCs, which include hydrocarbons, aldehydes, ketones, alcohols, esters, aromatics and sulfides (Statheropoulos et al. 2005). For example, *L. sericata* is preferentially attracted to the VOCs dimethyl disulfide (DMDS) and butan-1-ol (Frederickx et al. 2012).

Some of the VOCs are quorum-sensing compounds that can serve as attraction and oviposition cues to the colonizing insects and also signify the resource quality of the remains (Ma et al. 2012, Tomberlin et al. 2012, Liu et al. 2016). *L. sericata* showed increased attraction and oviposition when exposed to the wild type bacteria *Proteus mirabilis* with the ability to swarm as opposed to a non-swarming strain of the bacteria (Ma et al. 2012). The ability of arthropods to exhibit behavioral changes in response to compounds associated with microbial activity and behavior is a proposed mechanism arthropods use to evaluate the quality of the carrion resource (Tomberlin et al. 2012).

Volatile organic compounds produced by wound-isolated bacteria differentially attract female screwworms *Cochliomyia hominivorax* (Coquerel) (Diptera: Calliphoridae) for oviposition depending on the incubation time of the bacteria and also the amount and type of bacterial species present (Chaudhury et al. 2010). A complex relationship between stimulus and response is indicated by volatiles from substrates with more bacterial species present and volatiles from 48 and 72 h incubation times resulting in significantly more attraction and oviposition of the female screwworm (Chaudhury et al. 2010).

Interactions Between Microbes and Insects

In many instances, bacteria and fly larvae compete for carrion-associated resources. Mechanisms such as nutrient alteration and production of antibiotics and toxins are highlighted as factors in the coevolution and coexistence of microbes,

vertebrates, and rich food sources (Janzen 1977). Some arthropods associated with carrion produce antibiotics, exhibit antimicrobial strategies or evolve to be successful in the presence of microbes (Rozen et al. 2008, Cazander et al. 2009a, Cerovsky et al. 2010, Diaz-Roa et al. 2014). Microbes, with strategies of their own, can also become successful at the expense of other colonizing organisms by producing VOCs that deter colonization and repel other organisms (Janzen 1977, Deron et al. 2006, Andersen et al. 2010a).

Physical and biochemical interactions between microbes and insects are of interest to the forensic and medical fields. In the case of forensics, microbial communities in carrion can affect the response of colonizing blow flies (Peleg et al. 2008, Tomberlin et al. 2012), which could in turn impact the PMI determination. Identifying these biochemical markers produced by microbes and insects alike could lead to the discovery of novel antimicrobial compounds (Cerovsky et al. 2010).

Metagenomic Analysis

Metagenomic examination of the relationships between bacteria associated with wounds on human hosts is of particular importance due to the prevalence of multi drug resistant bacterial strains. Improved sequencing and gene expression analysis methods (Shendure and Ji 2008) combined with more powerful data analysis tools allow a more in-depth examination of the biochemical interactions between bacteria and blow flies like *L. sericata*. The gene expression response of *L. sericata* to a variety of factors can

be evaluated with the aid of the previously assembled transcriptome for this species (Sze et al. 2012). Gene expression analysis has been examined in *L. sericata* for the antimicrobial compound lucifensin (Valachova et al. 2013), as well as temporal gene expression analysis in the development of forensically relevant blow flies (Tarone and Foran 2011, Boehme et al. 2014). The availability of large data sets for comparative studies, as well as the use of RNA-sequencing technology and data analysis tools will support and aid gene expression studies in *L. sericata*.

Medical and Economic Threat of Drug Resistant Pathogens

The decreasing investment in antibacterial drug development coupled with the increase in antimicrobial resistance could lead to a future medical and socio-economic catastrophe (Chopra et al. 2008, Boucher et al. 2009, Lawrence and Jeyakumar 2013). Demographic trends in developed countries combined with advancements in medical care lead to a growing number of elderly patients and patients undergoing surgery, transplantation, chemotherapy, and neonatal intensive care (Chopra et al. 2008, Boucher et al. 2009). These demographic and patient trends produce an even greater number of vulnerable and immunocompromised individuals at risk of nosocomial infections (Chopra et al. 2008). The health care costs for patients with antibiotic-resistant nosocomial infections are substantial (Wilson et al. 2004, Chopra et al. 2008). Wilson et al. (2004) reported that the hospital cost for treating a patient with severe burns was on average $98,575 higher if they acquired a multi-drug resistant *Acinetobacter baumannii*

infection as compared to control patients. Resistance to first-line agents often results in administration of less satisfactory and sometimes toxic drugs, with an associated increase in the length of hospital stay and other complications (Chopra et al. 2008).

Drug resistant bacteria threaten public safety, and concern has been expressed for over 20 years (Harrison and Lederberg 1998, Wise et al. 1998, Livermore 2003, Beovic 2006, Talbot et al. 2006). Despite the overwhelming amount of knowledge and concern, there still has not been an adequate response to this threat (Livermore 2003, Boucher et al. 2009, Lawrence and Jeyakumar 2013). This limitation is due to drug development being difficult, costly, and time consuming; however, new antimicrobials are needed to treat infections caused by ESKAPE (*Enterococcus faecium, Staphylococcus aureus, Klebsiella pneumoniae, A. baumannii, Pseudomonas aeruginosa, Enterobacter* spp.) pathogens that currently cause the majority of hospital infections and effectively "escape" the effects of antibacterial drugs (Talbot et al. 2006, Boucher et al. 2009, Lawrence and Jeyakumar 2013). Additionally, panantibiotic-resistant infections now occur and several highly resistant Gram-negative bacteria, including *Acinetobacter* and *Pseudomonas* species, are emerging as significant pathogens in both the United States and other parts of the world (Chopra et al. 2008, Boucher et al. 2009).

Bacteria can become drug resistant from target site modifications or from functional bypassing of that target (Livermore 2003). Resistance can be contingent on impermeability, efflux, or enzymatic inactivation. If resistance is not inherent, then it may arise due to biofilm formation, mutation, or DNA transfer by plasmids, transposons and lysogenic bacteriophage (Davies et al. 1998, Livermore 2003, Beovic 2006,

Birkenhauer et al. 2014). As summarized by Livermore (2003), antibacterial agents may actually cause the emergence of variants with an increased propensity to develop further resistance. These hypermutators have up to 200-fold higher mutation rate than normal cells and so are more likely to become resistant to a first encounter with an antibacterial drug. Once selected by this first drug, they are then "primed" to develop resistance to subsequent antibacterial agents (Livermore 2003). In an effort to combat multi-drug resistant pathogens, there is a great need to provide funding for new research, develop alternative antibiotic approaches, as well as provide monetary incentives for drug companies to pursue antibiotic drug development (Boucher et al. 2009, Lawrence and Jeyakumar 2013).

Maggot Debridement Therapy and Success of L. sericata

Maggot debridement therapy (MDT), a drug alternative approach, is essentially a controlled and therapeutic maggot infestation of a wound that aids in debridement, disinfection, and cleaning (Sherman 2014). Live fly larvae, typically disinfected *L. sericata*, are applied to wounds with a special dressing and help remove dead and infected tissue and debris, stimulating new growth and healthy tissue formation (Baer 1931, Sherman 2014). Baer (1931) began extensive clinical research with MDT after marveling at the condition of wounds in two soldiers that had sustained compound fractures of the femur. The soldiers lay wounded for seven days with no food or water and their wounds were heavily infested with maggots. The wounds and the health of the

soldiers were in excellent condition with evidence of new tissue growth and no signs of infection. Baer (1931) also focused his efforts on rearing sterile maggots so they could be applied to wounds without causing detrimental effects to the patient. Blow fly larvae were applied and deemed successful in healing wounds in patients with chronic osteomyelitis (Baer 1931). Although the beneficial effects of maggots in wounds has been reported since the 16th century (Goldstein 1931), it was Baer (1931) that developed the proper methods to study the application of blow fly larvae to wounds in a clinical setting (ScienceNews 1931, Sherman et al. 2000).

Lucilia sericata larvae successfully debride, disinfect, and stimulate growth of new tissue and healing in wounds (Baer 1931, Nigam et al. 2006, Sherman 2014). The digestive enzymes that the larvae secrete and excrete, as well as the physical and scraping movement of the larvae across the wound, contribute to the debridement of necrotic tissue (Chambers et al. 2003, Sherman 2014). Larvae disinfect wounds in part by physically moving across the wound and disrupting biofilm formation and also by ingesting microbes (Mumcuoglu et al. 2001, Sherman 2014). Larvae secrete antimicrobial compounds that inhibit the growth of bacteria (Daeschlein et al. 2007, Bexfield et al. 2008, Cazander et al. 2009b, Cerovsky et al. 2010, Teh et al. 2013) and disrupt the formation of biofilms (Cazander et al. 2009a, Cazander et al. 2010, Bohova et al. 2014). MDT stimulates new tissue growth and wound healing in clinical settings (Baer 1931, Mumcuoglu et al. 1998, Nigam et al. 2006). Larvae also produce compounds that decrease the generation of pro-inflammatory factors and have a

beneficial effect on wound healing by regulating the inflammatory response (van der Plas et al. 2009, Cazander et al. 2012).

Objectives and Hypothesis

To analyze gene expression of medical-grade *L. sericata* 2nd instar exposed to *Pseudomonas aeruginosa* and *Acinetobacter baumannii* bacteria (test group) and those larvae not exposed (control group).

H_0: No difference detected in the level of gene expression between the test and control group larvae.

H_1: Differential gene expression occurs between test and control group larvae.

Rationale/Justification:

There is an urgent need to discover new mechanisms to overcome antibiotic resistant pathogens. Specifically, *A. baumannii* and *P. aeruginosa* are amongst the most challenging and resistant pathogens encountered in the hospital, battlefield, and natural disaster setting (Maragakis and Perl 2008, Peleg et al. 2008, Mihu and Martinez 2011, O'Shea 2012, Biswal et al. 2014). *Acinetobacter, Enterobacter* species, and *P. aeruginosa* were identified most frequently from infections associated with combat acquired type III open tibia fractures in a group of soldiers serving in Iraq and Afghanistan (Johnson et al. 2007).

Treatment of infected wounds with *L. sericata* larvae can be successful (Sherman 2002, Cazander et al. 2013). Antimicrobial activity by the larvae is one of the

mechanisms by which *L. sericata* controls wound pathogens (Daeschlein et al. 2007, Cazander et al. 2009b, Cerovsky et al. 2010, Bohova et al. 2014). Lucifensin is an example of a well-characterized antibacterial substance that is found in the excretions/secretions of these larvae (Andersen et al. 2010b, Cerovsky et al. 2010, Valachova et al. 2013, Valachova et al. 2014).

There is justification for further examination of the biochemical interactions that are taking place between the bacterial pathogens and the larvae. Exposing larvae to the chosen strains of bacteria and examining genes that are differentially expressed can potentially lead to the discovery of novel antimicrobial products. Gene expression analysis has progressed with improvements in sequencing technology, as well as data analysis methods and technology. Also, with decreased sequencing costs, more genomic and transcriptomic sequencing data is becoming available for non-model organisms. This project will also contribute to the growing amount of sequencing data that is available for this medically and forensically important species, *L. sericata*.

CHAPTER II

RESEARCH, RESULTS, AND DISCUSSION

Introduction

Without policies to stop the spread of antimicrobial resistance, there could be 10 million deaths globally annually by 2050 (O'Neill 2016). The economic cost of antimicrobial resistance will also continue to grow and could become an estimated 100 trillion USD by the year 2050 (O'Neill 2016). At least two million people in the US become infected with antibiotic resistant bacteria annually, and at least 23,000 people die each year as a direct result (Centers for Disease Control and Prevention 2017). Based on 2014 data for acute care hospitals, approximately one in 25 U.S. patients will contract at least one infection during the course of their hospital stay (Centers for Disease Control and Prevention 2016).

Antibiotics represent 4.5% of the global pharmaceutical market and is expected to have a 2% increase in compound annual growth rate (CAGR) by 2020 (Newswire 2016). Main drivers for the increase in CAGR are an aging population, rise in infectious diseases, increased prevalence of hospital-acquired infections, and new drug launches (Newswire 2016). While there are incentives for pharmaceutical companies to develop antibiotics, most newly developed compounds are lacking in biological innovation and public health benefit (Doshi 2015) as they are extensions to already existing drug classes

(Deak et al. 2016). Thus, emphasis should be placed on the development of novel compounds and innovative methods to overcome microbial infections.

New antimicrobials are needed to treat infections caused by ESKAPE (*E. faecium, S. aureus, K. pneumoniae, A. baumannii, P. aeruginosa, Enterobacter* spp.) pathogens that currently cause the majority of hospital infections and effectively "escape" the effects of antibacterial drugs (Talbot et al. 2006, Boucher et al. 2009, Lawrence and Jeyakumar 2013). Highly resistant Gram-negative pathogens are emerging as significant pathogens in both the US and other parts of the world (Chopra et al. 2008, Boucher et al. 2009).

As a potential source of novel antibiotics, *L. sericata* larvae have drawn attention due to their successful use in wound therapy as medical maggots. These larvae successfully debride, disinfect, and stimulate growth of new tissue and healing in wounds (Baer 1931, Nigam et al. 2006, Sherman 2014). The digestive enzymes the larvae secrete and excrete, as well as their physical and scraping movement across the wound, contribute to the debridement of necrotic tissue (Chambers et al. 2003, Sherman 2014). Larvae also secrete antimicrobial compounds (Daeschlein et al. 2007, Bexfield et al. 2008, Cazander et al. 2009b, Cerovsky et al. 2010, Teh et al. 2013), disrupt the formation of biofilms (Cazander et al. 2009a, Cazander et al. 2010, Bohova et al. 2014), and produce anti-inflammatory factors that have a beneficial effect on wound healing by regulating the inflammatory response (van der Plas et al. 2009, Cazander et al. 2012).

The insect innate immune system has remarkable plasticity due in part to the unique selection pressures of different ecological niches (Vilcinskas 2013). A diverse

repertoire of antimicrobial peptides is expected for insects that prosper in contaminated environments. The transcriptome of *L. sericata* contains 47 genes that encode putative antimicrobial peptides and small proteins, which is the second largest number of these peptides reported thus far in a multicellular organism (Pöppel et al. 2015). Analysis of the transcriptome with high throughput RNA sequencing (RNA-Seq) provides a mechanism to examine and discover genes. The gene expression response of *L. sericata* can be evaluated with the aid of the previously assembled transcriptome (Sze et al. 2012) and with the published genome for a closely related species, *Lucilia cuprina* (Wiedemann) (Diptera: Calliphoridae) (Anstead et al. 2015). The gene expression in *L. sericata* for the antimicrobial compound lucifensin (Valachova et al. 2013) has been examined along with temporal gene expression in the development of forensically relevant blow flies (Tarone and Foran 2011, Boehme et al. 2014). In this study, differential expression analysis was conducted on the transcripts from medical-grade *L. sericata* larvae exposed to *A. baumannii* and *P. aeruginosa* to potentially identify genes that encode beneficial peptides in response to harmful pathogens.

Materials and Methods

Acquisition and Preparation of Bacteria

The bacterial strains used were *Pseudomonas aeruginosa* (Schroeter) Migula (ATCC® 15692™; American Type Culture Collection, Manassas, Virginia) isolated

from an infected wound and *Acinetobacter baumannii* Bouvet and Grimont (ATCC® 19606™) isolated from urine.

The bacteria were prepared and stored at -80°C according to manufacturer's instructions. The bacteria were cultured on Trypticase Soy Agar (TSA) 24 h in advance and single colonies were isolated and passaged onto new TSA plates incubated 18-24 h at 37°C. The inoculum was brought to a 0.7 OD_{600nm} in phosphate buffered saline and placed on ice until use. The inoculum was enumerated by a tenfold serial dilution in PBS spread onto TSA plates and incubated 18-24 h at 37°C.

Arrival and Preparation of Medical Maggots

MedicalMaggots™ *L. sericata* larvae were supplied by Monarch Labs (Irvine, CA). Disinfected eggs were impregnated in sterile gauze and shipped overnight. Upon arrival, larvae were examined and verified to be second instar, an approximate count was performed, and a small collection of larvae was placed in Trypticase Soy Broth (TSB) and incubated at 37°C overnight and monitored for bacterial growth. Larvae were aseptically removed from the shipping vial and 15 larvae were aliquoted into each treatment tube.

Exposure tubes consisted of 10 µL of bacterial inoculum added onto a slant of 2 mL of TSA in 5 mL round bottom polypropylene tubes (Thermo Fisher Scientific Inc., Wilmington, Delaware), see Fig. 1. Eight replicate treatment tubes were prepared for each bacterial concentration and control tubes were prepared by adding 10 µL PBS. The tubes were incubated at room temperature for 30 minutes in the biosafety hood prior to

use. Larvae (15) were then aseptically added to each tube, which was capped and incubated at room temperature in the biosafety hood.

Collection of Larvae After Exposure Time Points

A summary of samples collected for the experiment is provided in Table 1.

Table 1 List of Sample Names

	Larval Stage Used:		2nd	1st	2nd	2nd
Treatment	Exposure (h)	Replicate	Experiment 1 Sample Identifier	Experiment 2 Sample Identifier	Experiment 3 Sample Identifier	Experiment 4 Sample Identifier
PBS (control)	1	A	C1A1	C1A2	C1A3	C1A4
		B	C1B1	C1B2	C1B3	C1B4
		C	C1C1	C1C2	C1C3	C1C4
		D	C1D1	C1D2	C1D3	C1D4
P. aeruginosa	1	A	PA1A1	PA1A2	PA1A3	PA1A4
		B	PA1B1	PA1B2	PA1B3	PA1B4
		C	PA1C1	PA1C2	PA1C3	PA1C4
		D	PA1D1	PA1D2	PA1D3	PA1D4
A. baumannii	1	A	AB1A1	AB1A2	AB1A3	AB1A4
		B	AB1B1	AB1B2	AB1B3	AB1B4
		C	AB1C1	AB1C2	AB1C3	AB1C4
		D	AB1D1	AB1D2	AB1D3	AB1D4
PBS (control)	4	A	C4A1	C4A2	C4A3	C4A4
		B	C4B1	C4B2	C4B3	C4B4
		C	C4C1	C4C2	C4C3	C4C4
		D	C4D1	C4D2	C4D3	C4D4
P. aeruginosa	4	A	PA4A1	PA4A2	PA4A3	PA4A4
		B	PA4B1	PA4B2	PA4B3	PA4B4
		C	PA4C1	PA4C2	PA4C3	PA4C4
		D	PA4D1	PA4D2	PA4D3	PA4D4
A. baumannii	4	A	AB4A1	AB4A2	AB4A3	AB4A4
		B	AB4B1	AB4B2	AB4B3	AB4B4
		C	AB4C1	AB4C2	AB4C3	AB4C4
		D	AB4D1	AB4D2	AB4D3	AB4D4

After 1 and 4 h, larvae from 4 control tubes and 8 treatment tubes (4 tubes for *P. aeruginosa* and 4 for *A. baumannii*) were sterilely collected. Ten larvae from each collection were placed into a 1.5 mL microcentrifuge tube (Thermo Fisher Scientific

Inc., Wilmington, Delaware) and immediately placed in an isopronol/dry ice mixture to flash freeze the larvae, then stored at -80°C for subsequent RNA analysis. The remaining 5 larvae were collected and externally sterilized by serial immersion in 1 mL of ethanol followed by SporGon (Decon Laboratories Inc., Sussex, UK) (Crippen and Sheffield 2006). The tube was gently shaken for 3 min, then the ethanol or Sporgon drained using a sterile barrier screen. Larvae were then transferred aseptically to a new tube containing sterile H_2O and left for 1 min, drained, and transferred to a 14 mL centrifuge tube containing 1.5 mL sterile PBS. The larvae were then homogenized using a sonicator-model 8851-34 (Cole Parmer, Vernon Hills, IL). The homogenate was serially diluted by a 10 fold dilution to 10^{-6} in PBS and plated onto TSA plates; incubated 18-24 hr at 37°C, and enumerated. Remaining homogenate volume was stored at -20°C. The experiment was repeated on four separate days. The larvae in experiment 2 were identified as being first instar and the total number of larvae was limited, so only the bacterial exposure portion of the experiment was carried out and no RNA analysis was done. For this group, approximately 15 larvae per sample were collected.

RNA Extraction and Sequencing

For RNA extraction, five larvae were removed from each 1.5 mL microcentrifuge tube and placed in a new 1.5 mL microcentrifuge tube. All tubes and consumables were RNAse-free. RNA was extracted in a two-step process. First, whole RNA was extracted using TriReagent (Sigma-Aldrich Corp., St. Louis, Missouri) preparation according to manufacturer's protocols. Briefly, one sample (~5 whole larvae) was macerated in 1 mL of cold TriReagent. Following this, 50 mL of ice-cold

BAN reagent (Molecular Research Center, Inc., Cincinnati, Ohio) was added and the solution was vigorously mixed. Next, the tubes were centrifuged at 14,000 G at 4°C for 15 minutes to isolate the RNA from the DNA and proteins. Approximately 500 µL of the top clear layer was carefully removed with a pipet and added to 500 µL of ice-cold 100% isopropanol. The tubes were mixed via inversion three times and allowed to rest on ice for 10 min to precipitate the RNA. The precipitate was then centrifuged at 14,000 G at 4°C for 15 min. Next, the supernatant was completely removed, 1 mL of ice-cold 70% ethanol was used to wash the RNA pellet, and the pellet was centrifuged at 4°C for 5 min at 14,000 G. The ethanol was eluted, and any remaining ethanol was allowed to completely evaporate. The RNA was then dissolved in a 10µL mixture of 99 µL of DNase/RNase/Nucleotide-free water and 1 µL of SUPERase•In™ (Invitrogen, Life Technologies Incorporated, Grand Island, New York).

For the second step, the extracted RNA was further purified using a Qiagen RNeasy Micro Kit and on-column DNase treatment following manufacturer protocols (Qiagen Inc., Valencia, California). RNA was eluted again into a fresh 1:100µL mixture of SUPERase•In and DNase/RNase/Nucleotide-free water and stored at -80°C until sequencing.

Sample concentration and quality was assessed with NanoDrop (Thermo Fisher Scientific Inc., Wilmington, Delaware) and an Agilent 2100 BioAnalyzer (Agilent Technologies Inc., Santa Clara, California). In total, 72 paired-end libraries were multiplexed and sequenced on six separate RNA HiSeq flow cells. RNA was sequenced on an Illumina Hi-Seq 2500 (Illumina, Inc., San Diego, California) following

manufacturer protocols regarding library preparation. All sequencing was performed by the Genomics and Bioinformatics Services at Texas A&M AgriLife Research (College Station, TX). Sequence cluster identification, quality prefiltering, base calling and uncertainty assessment were done in real time using Illumina's HCS 2.2.68 and RTA 1.18.66.3 software with default parameter settings. Sequencer.bcl basecall files were demultiplexed and formatted into .fastq files using bcl2fastq 2.17.1.14 script configureBclToFastq.pl.

Data Analysis

Sequencing data was downloaded from the Texas Agrilife Research website https://download.txgen.tamu.edu with project specific credentials. The sequencing files, reference genomes, and applicable programs were uploaded to the Texas A&M Institute for Genome Sciences and Society (TIGSS) HPC Cluster. The HPC cluster provides computational resources and systems administration support to allow data analysis and storage solutions for large data sets.

The sequencing reads were first aligned to the published *L. cuprina* reference genome (Anstead et al. 2015) which includes a transcriptome for which there are 14,452 annotated genes. For alignment, the program TopHat v2.1.1 (Trapnell et al. 2009) was used to map reads to the genome. Sequence alignment to the *L. sericata* genome was also performed to see if it would improve the alignment rate. No further analysis was performed due to the lack of a compatible annotation file. Mapped reads from the *L. cuprina* alignment output files were provided as input to the Cufflinks application (Trapnell et al. 2010) (http://cufflinks.cbcb.umd.edu/) which uses this map against the

genome to assemble the reads into transcripts (Trapnell et al. 2012). Cuffdiff (v2.2.1), a part of the Cufflinks package, takes the aligned reads from two or more conditions and reports genes and transcripts that are differentially expressed using a rigorous statistical analysis (Trapnell et al. 2012). Differential expression analysis was performed using the TopHat default settings and also with an increased mismatch rate and read-edit distance setting. Replicates within each day were treated as technical replicates and the four replicates (A-D) were added together for the Cuffdiff analysis. Each of the three experimental days (1, 3, and 4) were defined as biological replicates. Therefore, samples AB1A1-AB1D1, AB1A3-AB1D3, and AB1A4-AB1D4 would be incorporated as input into the analysis and the Cuffdiff output sample name would be AB1. Larvae exposed to *A. baumannii* for 1 h represent the AB1 group and C1 is the corresponding control group. Larvae exposed to *A. baumannii* for 4 h represent the AB4 group and C4 is the corresponding control group. Larvae exposed to *P. aeruginosa* for 1 h represent the PA1 group and C1 is the corresponding control group. Lastly, larvae exposed to *P. aeruginosa* for 4 h represent the PA4 group and C4 is the corresponding control group.

Since longer transcripts are more likely to have reads mapped to them, correction for transcript length bias is carried out in Cuffdiff with the use of normalized FPKM (fragments per kilobase of transcript per one million mapped reads) values (Trapnell et al. 2012). Cuffdiff output expression data files were indexed and visualized using R v3.2.4 (R Core Team 2016) and the CummeRbund v2.12.1 (http://compbio.mit.edu/cummeRbund/) package to facilitate exploration of genes identified by Cuffdiff as differentially expressed (Trapnell et al. 2012). The cut-off for

determining significant differential expression was an adjusted P value (Q value) $\leq$ 0.05 from the Cuffdiff output. Genes from each type of analysis that were differentially expressed at a significant level were compared using an online tool (Oliveros 2007-2015) in order to determine if any identified genes were represented in more than one analysis set. Differential expression analysis was also explored with the DESeq2 v1.10.1 (Love et al. 2014) and Bioconductor v3.2 software packages (Gentleman et al. 2004).

Gene Ontology

The functional roles of differentially expressed protein products were identified by various methods. First, differentially expressed genes with *L. cuprina* gene names were researched in the Ensembl Metazoa database (Kersey et al. 2016) and also with the use of the InterPro (Finn et al. 2016) and the UniProt (The UniProt Consortium 2014) databases. The BioMart portion of Ensembl (Kinsella et al. 2011) was used to assign alternative gene names to the identified *L. cuprina* significant differentially expressed genes. Another method involved comparing identified genes to those found in *Drosophila melanogaster* Meigen (Diptera: Drosophilidae) data in http://www.flybase.org (Gelbart and Emmert 2010). The nodes of the transcriptome were also compared against characterized proteins from other organisms using a translated Basic Local Alignment Search Tool (BLAST) search (Altschul et al. 1990). After assigning functions and characterizing protein products of differentially expressed genes, some gene sets were further analyzed using the Panther database and gene enrichment software tools (Thomas et al. 2006, Mi et al. 2016).

Results

Bacteria Exposure to *L. sericata* Larvae

Larvae (Medical Maggots™) that arrived from Monarch Labs did not produce bacterial growth when enriched overnight in TSB at 37°C. The starting inoculum concentrations for *A. baumanni* for the three biological experimental replicates ranged from 3.1 to 6.6 x 10^9 CFU/mL and for *P. aeruginosa* ranged from 0.5 to 1.5 x 10^{10} CFU/mL.

Larvae exposed to *A. baumanni* or *P. aeruginosa* had direct contact with the bacteria on the surface of the exposure tube where they typically either remained or burrowed slightly into the agar (Fig. 1).

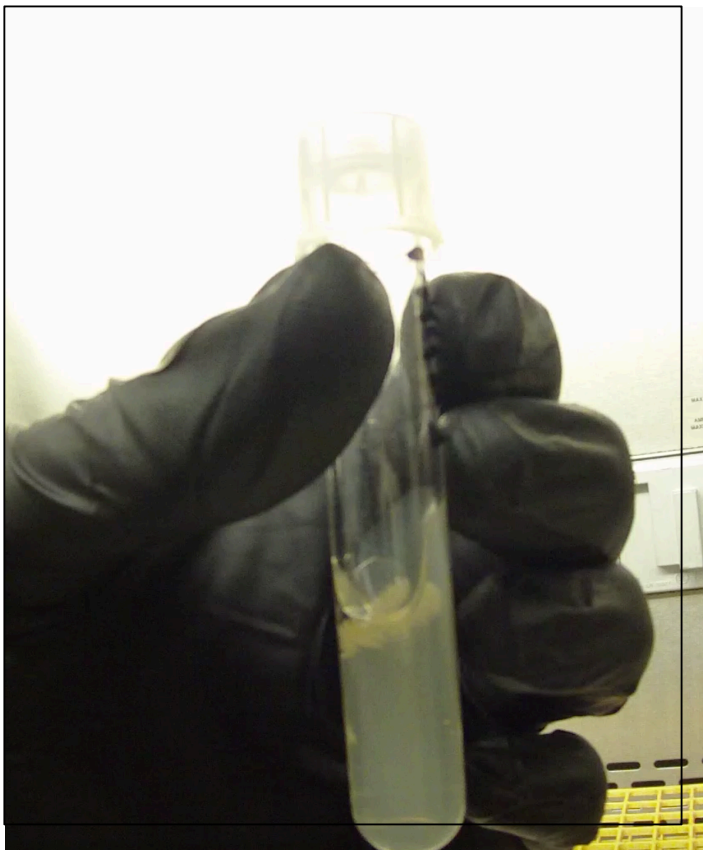

Fig. 1: Larvae just below surface of agar in 5 mL round bottom tube.

Only live larvae were collected during the experiment. Larvae that were exposed to PBS did not produce bacterial growth and larvae exposed to *A. baumannii* or *P. aeruginosa* produced bacterial colonies phenotypically similar to the respective species.

Three larvae each were individually enriched overnight in TSB at 37°C after exposure to either *A. baumannii* and *P. aeruginosa* and external disinfection . Larvae showed no signs of bacterial growth with the exception of one larva post *P. aeruginosa* exposure.

Cuffdiff Analysis with Default TopHat Parameters

Several genes were differentially expressed post *A. baumannii* or *P. aeruginosa* treatment of *L. sericata* larvae. Alignment of sequencing reads to the *L. cuprina* reference genome resulted in a 31.0% concordant pair alignment rate when default parameters were selected. Output diagnostics for a typical alignment using default TopHat parameters, which includes a mismatch rate setting of two, can be seen in Fig. 2.

```
Left reads:
          Input     :  13327997
           Mapped   :   5229242 (39.2% of input)
            of these:    132172 ( 2.5%) have multiple alignments
(136 have >20)
Right reads:
          Input     :  13327997
           Mapped   :   5512065 (41.4% of input)
            of these:    140284 ( 2.5%) have multiple alignments
(133 have >20)
40.3% overall read mapping rate.

Aligned pairs:   4211801
     of these:    105207 ( 2.5%) have multiple alignments
                   75713 ( 1.8%) are discordant alignments
31.0% concordant pair alignment rate.
```

Fig. 2: Example summary of TopHat alignment output with default parameters.

Table 2 presents a summary of Cuffdiff outputs with default TopHat parameters for AB1 compared to C1. A total of seven genes displayed significant differential expression ($Q \leq 0.05$) compared to the control when *L sericata* larvae were exposed to *A. baumannii* for 1 h. All seven of the identified genes (100%) were expressed at a lower level in the larvae exposed to *A. baumannii* as compared to the control (ie, no differentially expressed genes were upregulated). Gene FF38_12536, which is associated with an integral component of the plasma membrane, displayed the greatest fold change for a decrease in gene expression between C1 and AB1.

Table 3 presents a summary of Cuffdiff outputs with default TopHat parameters for PA1 compared to C1. A total of eight genes displayed significant differential expression ($Q \leq 0.05$) compared to the control when *L sericata* larvae were exposed to *P aeruginosa* for 1 h. Two of the eight differentially expressed genes (25%) were expressed at a higher level in the larvae exposed to *P. aeruginosa* as compared to the

control (ie, upregulated). Relative expression levels of the eight differentially expressed genes for PA1 vs C1 can be visualized in Fig. 3. Gene FF38_02709, which is an uncharacterized protein, had the greatest fold change in terms of increased gene expression between C1 and PA1. Gene FF38_12536, which is associated with an integral component of the plasma membrane, displayed the greatest fold change for a decrease in gene expression between C1 and PA1.

Table 2 Summary of Cuffdiff Output with Default TopHat Parameters (AB1 vs C1)

Gene	V1 (AB1)	V2 (C1)	Change[1]	Q value	EL	Gene Description
FF38_02450	9.1927	18.8507	1.03606	0.03753	Down	GO:0042302; structural constituent of cuticle[2]
FF38_14459	1.3011	13.4536	3.37018	0.03753	Down	Protein coding[3]
FF38_14465	0.5321	7.79236	3.87236	0.03753	Down	Protein coding[3]
FF38_12518	2.9482	6.75891	1.19698	0.03753	Down	GO:0016021; integral component of plasma membrane[2]; Dmel/Osiris2 [4]
FF38_12536	0.4469	7.24213	4.01832	0.03753	Down	Dmel/Osiris15: inferred, integral component of plasma membrane[4]
FF38_07366	0.497	1.22405	1.30034	0.03753	Down	GO:0004867; serine-type endopeptidase inhibitor activity[2]
FF38_00565	3.6553	7.99212	1.12857	0.03753	Down	Protein coding[3]

Abbreviations: AB1 = larvae exposed to *A. baumannii* for 1 h, C1 = control group larvae not exposed to bacteria for 1 h, EL = expression level, GO = Gene ontology GO term, V1 = Value 1, V2 = Value 2.

Note: Significant values defined as $Q \leq 0.05$.

[1] Change presented as log 2 (fold change) function.

Source: [2] InterPro, [3] EnsemblMetazoa, [4] FlyBase

Table 3 Summary Table of Cuffdiff Output with Default TopHat Parameters (PA1 vs C1)

Gene	V1 (PA1)	V2 (C1)	Change[1]	Q value	EL	Gene Description
FF38_02450	9.32128	19.3163	1.05122	0.033613	Down	GO:0042302; structural constituent of cuticle[2]
FF38_05420	4.79796	2.3866	-1.00746	0.033613	Up	GO:0016021; integral component of membrane[2]
FF38_14465	1.20161	7.99001	2.73324	0.033613	Down	Protein coding[3]
FF38_12536	0.3606	7.42597	4.36412	0.033613	Down	Dmel/Osiris15; inferred: integral component of plasma membrane[4]
FF38_02709	6.24286	2.25863	-1.46676	0.033613	Up	Protein coding[3]
FF38_03319	2.11099	13.7192	2.7002	0.033613	Down	Protein coding[3]
FF38_03322	0	1.06204	inf	0.033613	Down	Protein coding[3]
FF38_03381	13.0863	31.9503	1.28777	0.033613	Down	GO:0006030; chitin metabolic process, chitin binding[2]; Dmel/Peritrophin-15a/15b[4]

Abbreviations: PA1 = larvae exposed to *P. aeruginosa* for 1 h, C1 = control group larvae not exposed to bacteria for 1 h, EL = expression level, GO = Gene ontology GO term, V1 = Value 1, V2 = Value 2.

Note: Significant values defined as $Q \leq 0.05$.

[1] Change presented as log 2 (fold change) function.

Source: [2] InterPro, [3] EnsemblMetazoa, [4] FlyBase.

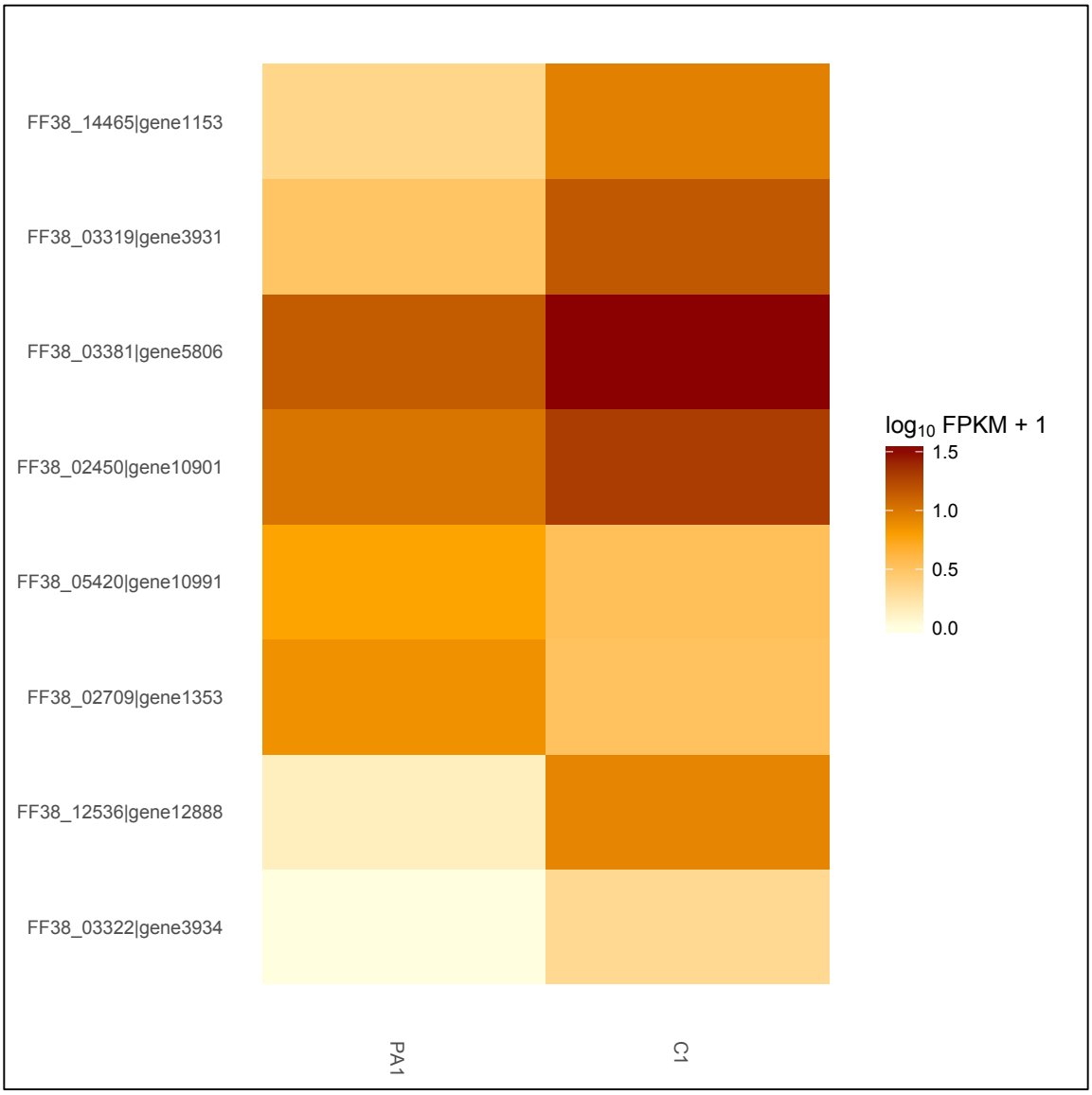

Fig. 3: Heatmap displaying relative expression levels of genes that are differentially expressed between larvae exposed to *P. aeuruginosa* for one hour (PA1) and control group larvae (C1). Expression levels between samples are compared in terms of log10 normalized mapped read (FPKM) values. Light beige coloring corresponds to lower levels of gene expression and dark orange coloring corresponds to higher levels of gene expression.

Table 4 presents a summary of Cuffdiff outputs with default TopHat parameters for AB4 compared to C4. A total of 28 genes displayed significant differential expression ($Q \leq 0.05$) compared to the control when *L sericata* larvae were exposed to

A. baumannii for 4 h. Twenty-one of the 28 differentially expressed genes (75%) were expressed at a higher level in the larvae exposed to *A. baumannii* as compared to the control (ie, upregulated). Genes FF38_02624 (uncharacterized protein) and FF38_01452 (peptidoglycan catabolic process) had the greatest fold change in terms of increased gene expression between C4 and AB4. Gene FF38_02709 (uncharacterized protein) displayed the greatest fold change in terms of decreased gene expression between C4 and AB4.

Table 5 presents a summary of Cuffdiff outputs with default TopHat parameters for PA4 compared to C4. A total of 13 genes displayed significant differential expression ($Q \leq 0.05$) compared to the control when *L sericata* larvae were exposed to *P. aeruginosa* for 4 h. Six of the 13 differentially expressed genes (46%) were expressed at a higher level in the larvae exposed to *P. aeruginosa* as compared to the control (ie, upregulated). Gene FF38_01452 (peptidoglycan catabolic process) had the greatest fold change for an increase in gene expression between C4 and PA4. Gene FF38_14459 (uncharacterized protein) displayed the greatest fold change for a decrease in gene expression between C4 and PA4.

Table 4 Summary Table of Cuffdiff Output with Default TopHat Parameters (AB4 vs C4)

Gene	V1 (AB4)	V2 (C4)	Change[1]	Q value	EL	Gene Description
FF38_00033	8.47366	12.3061	0.538313	0.0495804	Down	Protein coding[3]
FF38_02450	5.57209	3.46503	-0.685352	0.0115688	Up	GO:0042302: structural constituent of cuticle[2]
FF38_14459	4.80544	12.4898	1.37801	0.0115688	Down	Protein coding[3]
FF38_06989	30.697	18.8271	-0.705286	0.0115688	Up	Protein coding[3]
FF38_02624	773.001	299.65	-1.36719	0.0115688	Up	Protein coding[3]
FF38_02631	142.179	58.1401	-1.29011	0.0115688	Up	Protein coding[3]
FF38_10586	0.83048	0.34891	-1.25109	0.0115688	Up	GO:0035556: Intracellular signal transduction, GO:0046872: metal ion binding, GO:0005622: Intracellular[3]; Protein kinase C-like, phorbol ester/diacylglycerol-binding domain[2]
FF38_02709	4.69109	14.6275	1.64068	0.0115688	Down	Protein coding[3]
FF38_01452	89.3129	35.0482	-1.34953	0.0115688	Up	GO:0009253; peptidoglycan catabolic process (The chemical reactions and pathways resulting in the breakdown of peptidoglycans, any of a class of glycoconjugates found in bacterial cell walls), GO:0045087: innate immune response (Innate immune responses are defense responses mediated by germline encoded components that directly recognize components of potential pathogens)[2]
FF38_05096	1047.33	706.448	-0.568068	0.0115688	Up	GO:0042302: structural component of cuticle[2]
FF38_01073	2.97552	1.60363	-0.891802	0.0115688	Up	GO:0005515: Interacting selectively and non-covalently with any Protein or protein complex (a complex of two or more proteins that may include other non-protein molecules)[2]; Dmel/ecd, ecdysoneless[4]
FF38_03041	1.70961	0.936789	-0.867868	0.0115688	Up	GO:0005515; protein binding, Immunoglobulin-like domain[2]

Table 4 Continued

Gene	V1 (AB4)	V2 (C4)	Change[1]	Q value	EL	Gene Description
FF38_02640	2.19129	0.987594	-1.14979	0.0115688	Up	GO:0055114; oxidation-reduction process, TauD/TfdA-like domain[2]
FF38_12829	1.61703	0.815601	-0.987408	0.0115688	Up	GO:0035556: Intracellular signal transduction, GO:0046872: metal ion binding, GO:0005622: Intracellular; Protein kinase C-like, phorbol ester/diacylglycerol-binding domain[2]
FF38_02573	7.95852	5.30632	-0.584787	0.0320365	Up	protein coding[3]
FF38_07683	19.8311	28.6538	0.530962	0.0411333	Down	GO:0005509; calcium ion binding[2]
FF38_11848	12.115	5.10028	-1.24815	0.0115688	Up	Protein coding[3]
FF38_07690	4.48309	9.78556	1.12616	0.0115688	Down	Protein coding[3]
FF38_08124	16.9543	10.7624	-0.655655	0.0115688	Up	GO:0005576; extracellular region; transferrin like domain; Transferrins are a family of eukaryotic iron-binding glycoproteins that share the common function of controlling the level of free iron in biological fluids[2]
FF38_00377	2.23884	1.0181	-1.13687	0.0115688	Up	GO:004866; endopeptidase inhibitor activity[2]
FF38_05499	396.123	199.958	-0.986249	0.0115688	Up	Protein coding[3]
FF38_06625	1.24106	0	NA	0.0115688	Up	Protein coding[3]
FF38_14311	1.65819	2.86966	0.791275	0.0115688	Down	Protein coding[3]
FF38_14361	4.05522	2.21992	-0.869273	0.0115688	Up	GO:0006355: DNA-binding protein D-ETS-6 [2] ;GO:0003700: transcription factor activity, sequence-specific DNA binding[2]
FF38_00565	6.25318	3.94127	-0.665929	0.0115688	Up	Protein coding
FF38_02608	0.817969	0.500276	-0.709321	0.0320365	Up	Dmel/Tet: Contains 1 CXXC-type zinc finger; Oxygenase domain[4]

Table 4 Continued

Gene	V1 (AB4)	V2 (C4)	Change[1]	Q value	EL	Gene Description
FF38_03845	1.8576	1.05353	-0.818214	0.0115688	Up	GO:0007264: Rad and Gem related GTP binding protein 1; small GTPase mediated signal transduction[2]
FF38_04564	0.785602	0.443066	-0.826277	0.0115688	Up	GO:0034729: Histone-lysine N-methyltransferase, regulation of cell cycle[2]

Abbreviations: AB4 = larvae exposed to *A.* baumannii for 4 h, C4 = control group larvae not exposed to bacteria for 4 h, EL = expression level, GO = Gene ontology GO term, V1 = Value 1, V2 = Value 2.

Note: Significant values defined as $Q \leq 0.05$.

[1] Change presented as log 2 (fold change) function.

Source: [2] InterPro via EnsemblMetazoa, [3] EnsemblMetazoa, [4] FlyBase.

Table 5 Summary Table of Cuffdiff Output with Default TopHat Parameters (PA4 vs C4)

Gene	V1 (PA4)	V2 (C4)	Change[1]	Q value	EL	Gene Description
FF38_00033	7.50382	11.8137	0.654766	0.02719	Down	Protein coding[3]
FF38_14459	1.04258	12.0098	3.52598	0.02719	Down	Protein coding[3]
FF38_14466	0.470596	1.39336	1.56601	0.0418308	Down	Protein coding[3]
FF38_02624	73.6322	287.843	1.96687	0.02719	Down	Protein coding[3]
FF38_02631	15.1156	55.8479	1.88546	0.02719	Down	Protein coding[3]
FF38_02709	5.98234	14.0707	1.23391	0.02719	Down	Protein coding[3]
FF38_06525	8.58407	5.08942	-0.754161	0.0418308	Up	GO:0055114: oxidation-reduction process, GO:0016491: oxidoreductase activity[3]; TauD/TfdA-like domain[2]
FF38_06814	2.46444	4.48856	0.864991	0.0418308	Down	GO:0004252; serine-type endopeptidase activity[2]
FF38_01452	80.3626	33.63	-1.25677	0.02719	Up	GO:0008745: N-acetylmuramoyl-L-alanine amidase activity: Proteins containing this domain include zinc amidases that have N-acetylmuramoyl-L-alanine amidase activity EC:3.5.1.28. This enzyme domain cleaves the amide bond between N-acetylmuramoyl and L-amino acids in bacterial cell walls (preferentially: D-lactyl-L-Ala), GO:0008270: zinc ion binding, Peptidoglycan-recognition protein SB1 [5]
FF38_09514	7.19281	3.0444	-1.2404	0.02719	Up	GO:0005515: Kazal domain, serine proteinase inhibitors[2]
FF38_09769	2.5054	1.24238	-1.01194	0.02719	Up	GO:0005759; mitochondrial matrix, mitochondrial glycoprotein[2]
FF38_00377	2.3255	0.978874	-1.24834	0.02719	Up	GO:0004866; endopeptidase inhibitor activity, Alpha-2-macroglobulin, N-terminal[2]

Table 5 Continued

Gene	V1 (PA4)	V2 (C4)	Change[1]	Q value	EL	Gene Description
FF38_07809	29.8294	17.8153	-0.743617	0.02719	Up	Dmel\Lst: Limostatin (Lst) is a peptide hormone produced by endocrine corpora cardiaca cells during starvation. Lst suppresses insulin production and secretion from insulin-producing cells by signaling through the G-protein coupled receptor PK1-R[4]

Abbreviations: PA4 = larvae exposed to *P. aeruginosa* for 4 h, C4 = control group larvae not exposed to bacteria for 4 h, EL = expression level, GO = Gene ontology GO term, V1 = Value 1, V2 = Value 2.

Note: Significant values defined as $Q \leq 0.05$.

[1] Change presented as log 2 (fold change) function.

Source: [2] InterPro via EnsemblMetazoa, [3] EnsemblMetazoa, [4] FlyBase, [5] INSDC.

Pairwise comparisons of expression levels for all genes from Cuffdiff output is presented in Fig. 4 (AB4 vs C4) as well as in Fig. 5 (PA4 vs C4).

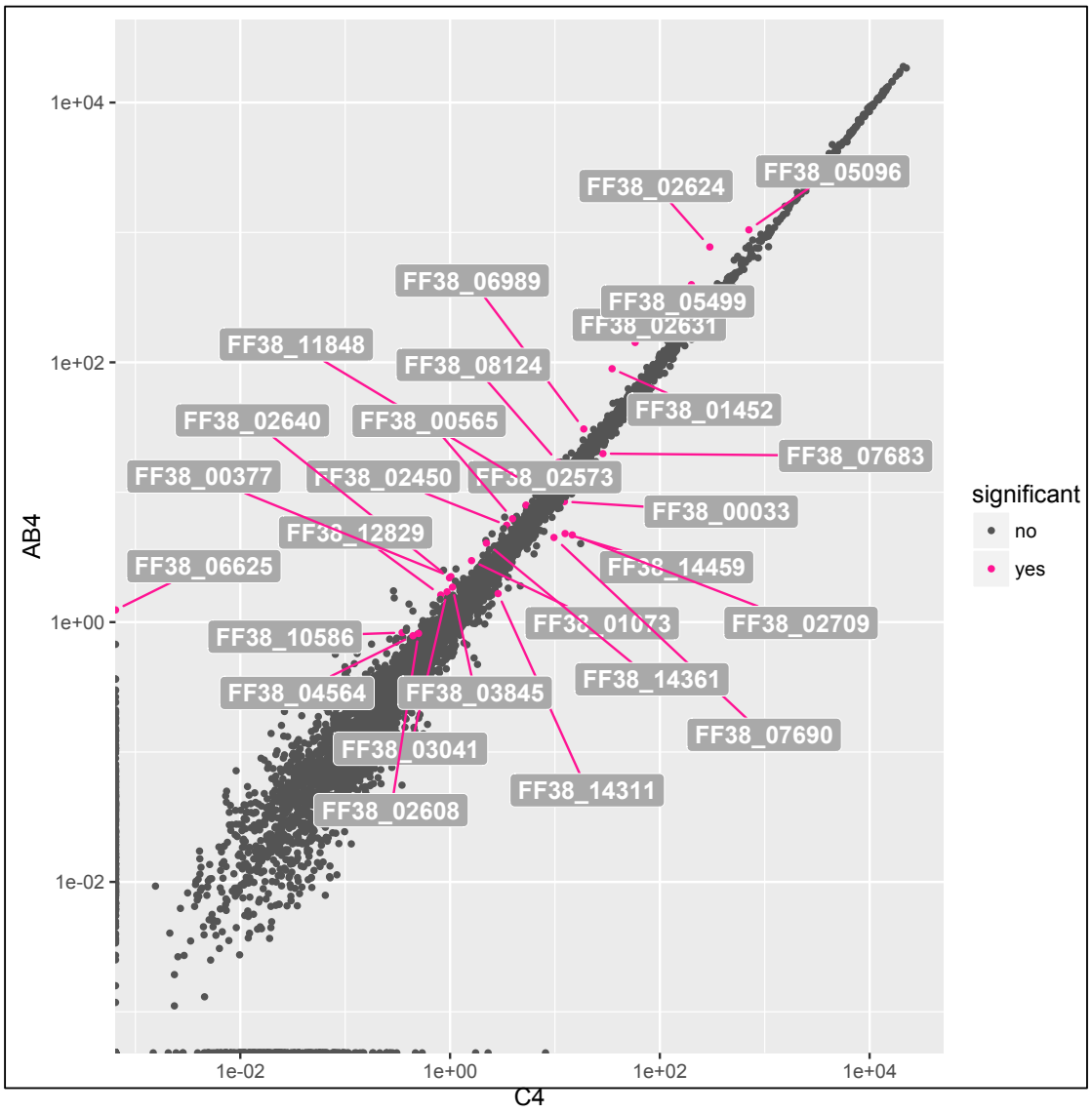

Fig. 4: Scatterplot of pairwise gene expression levels between AB4 and C4 with log10 transformed fpkm values. Genes that are differentially expressed at a significant level are highlighted and labeled. A data point above y=x represents a gene that is expressed at higher level in AB4 than in C4.

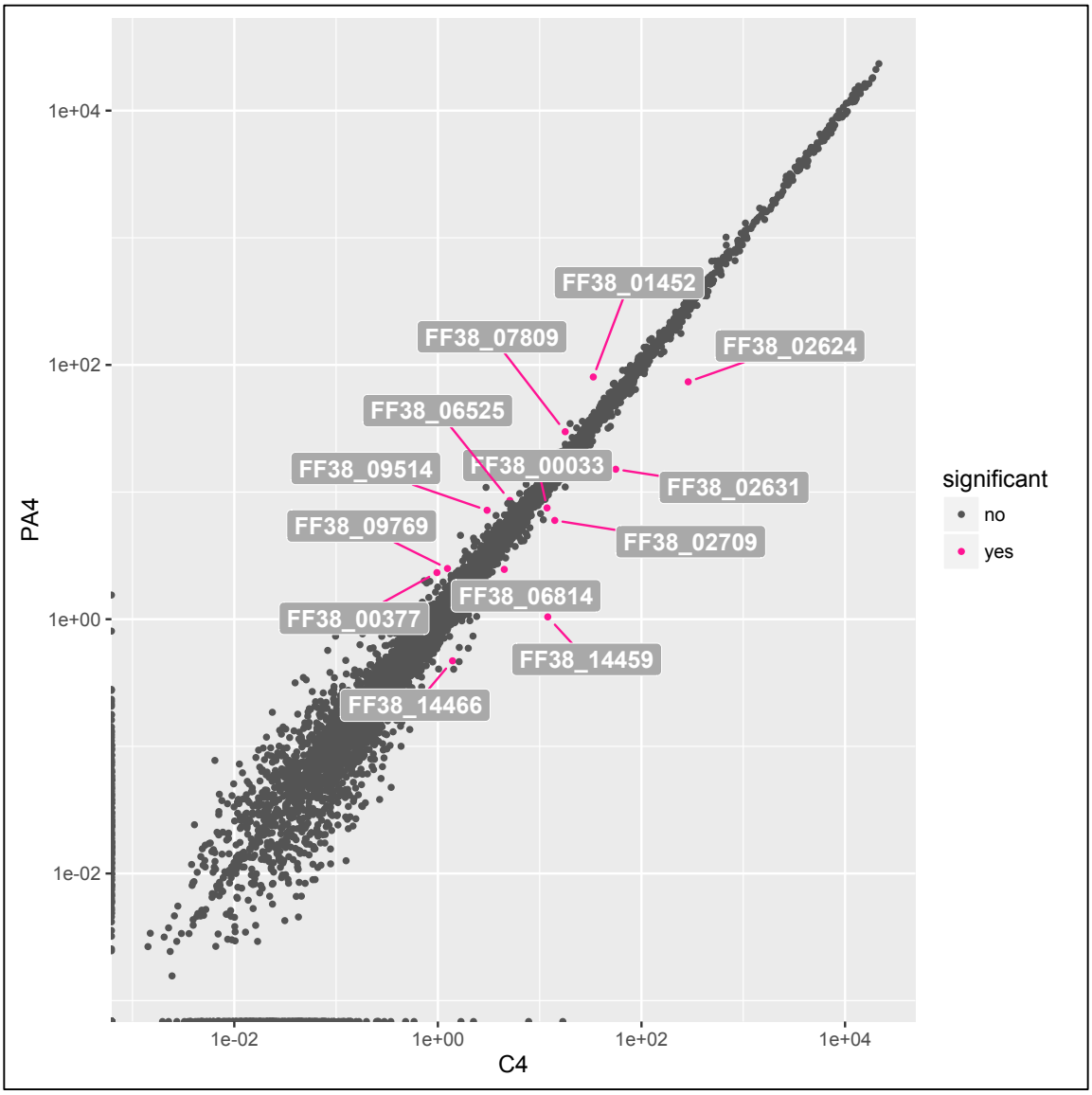

Fig. 5: Scatterplot of pairwise gene expression levels between PA4 and C4 with log10 transformed fpkm values. Genes that are differentially expressed at a significant level are highlighted and labeled. A data point above y=x represents a gene that is expressed at higher level in PA4 than in C4.

Six down-regulated differentially expressed genes were common to more than one analysis set; the Venn diagram in Fig. 6 presents the down-regulated significant differentially expressed genes as they appear in each Cuffdiff analysis performed with default TopHat parameters. The down-regulated genes FF38_02450, FF38_14465, and

FF38_12536 have similar patterns of expression in both AB1 vs C1 and PA1 vs C1. Gene FF38_02450 is associated with cuticle structure, gene FF38_14465 is protein coding (no identified function), and FF38_12536 is associated with an integral component of the plasma membrane. Genes FF38_00033 and FF38_02709, which are both uncharacterized proteins, were down-regulated in both AB4 vs C4 and PA4 vs C4. Gene FF38_14459 (uncharacterized protein) was found to be down-regulated in AB1 vs C1, AB4 vs C4, and PA4 vs C4. No down-regulated genes were represented in all four of the analysis sets.

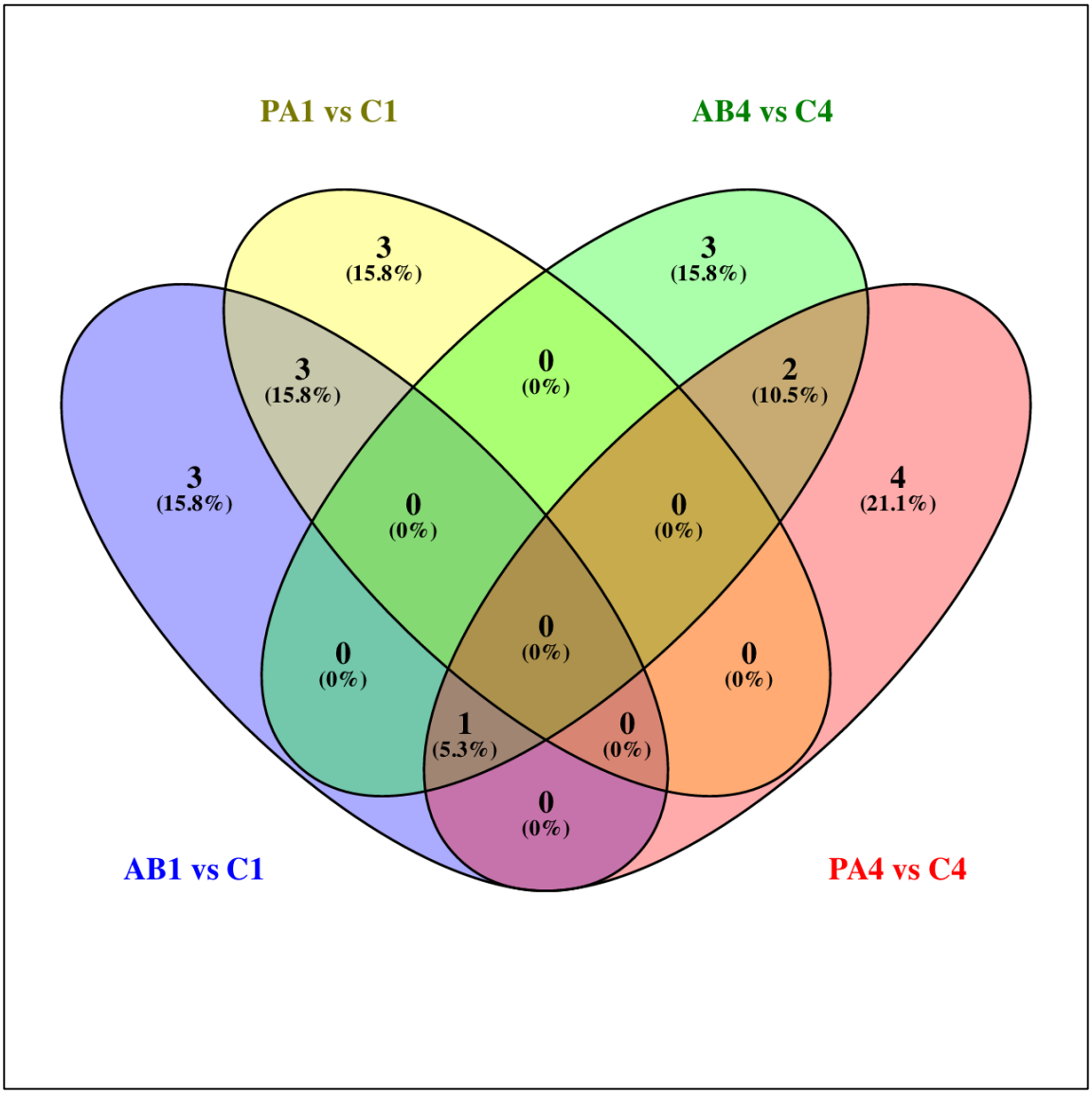

Fig. 6: Four-way Venn diagram displaying overlapping counts of significant differentially expressed genes that are down-regulated.

The up-regulated genes displaying significant differential expression from all Cuffdiff analysis sets are presented in the Venn diagram in Fig. 7. Gene FF38_00377 (endopeptidase inhibitor activity) and gene FF38_01452 (peptidoglycan catabolic

process) were found to be up-regulated in both AB4 vs C4 and PA4 vs C4. Expression levels displayed in barplot format for gene FF38_01452 can be examined in Fig. 8.

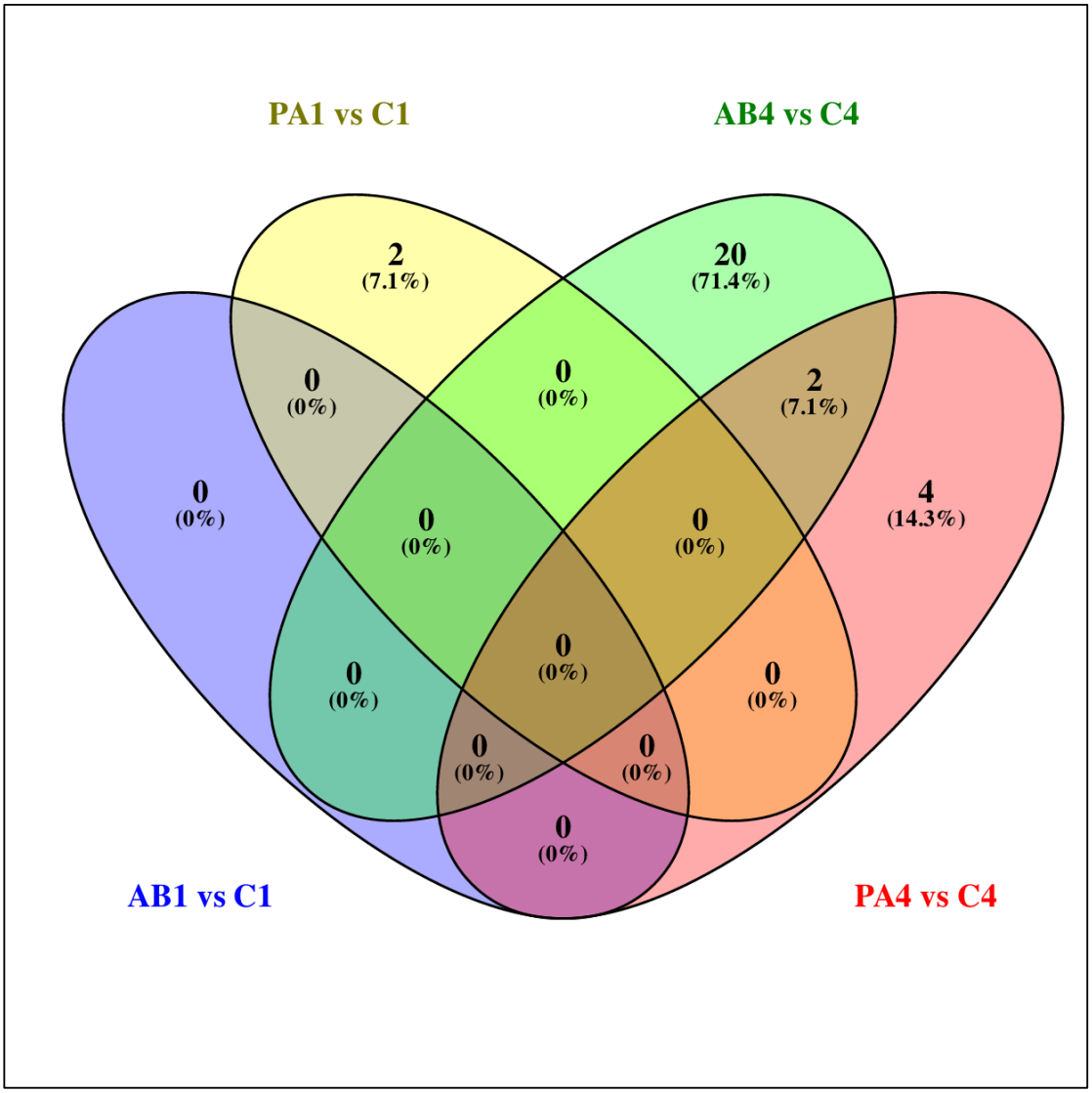

Fig. 7: Four-way Venn diagram displaying overlapping counts of significant differentially expressed genes that are up-regulated.

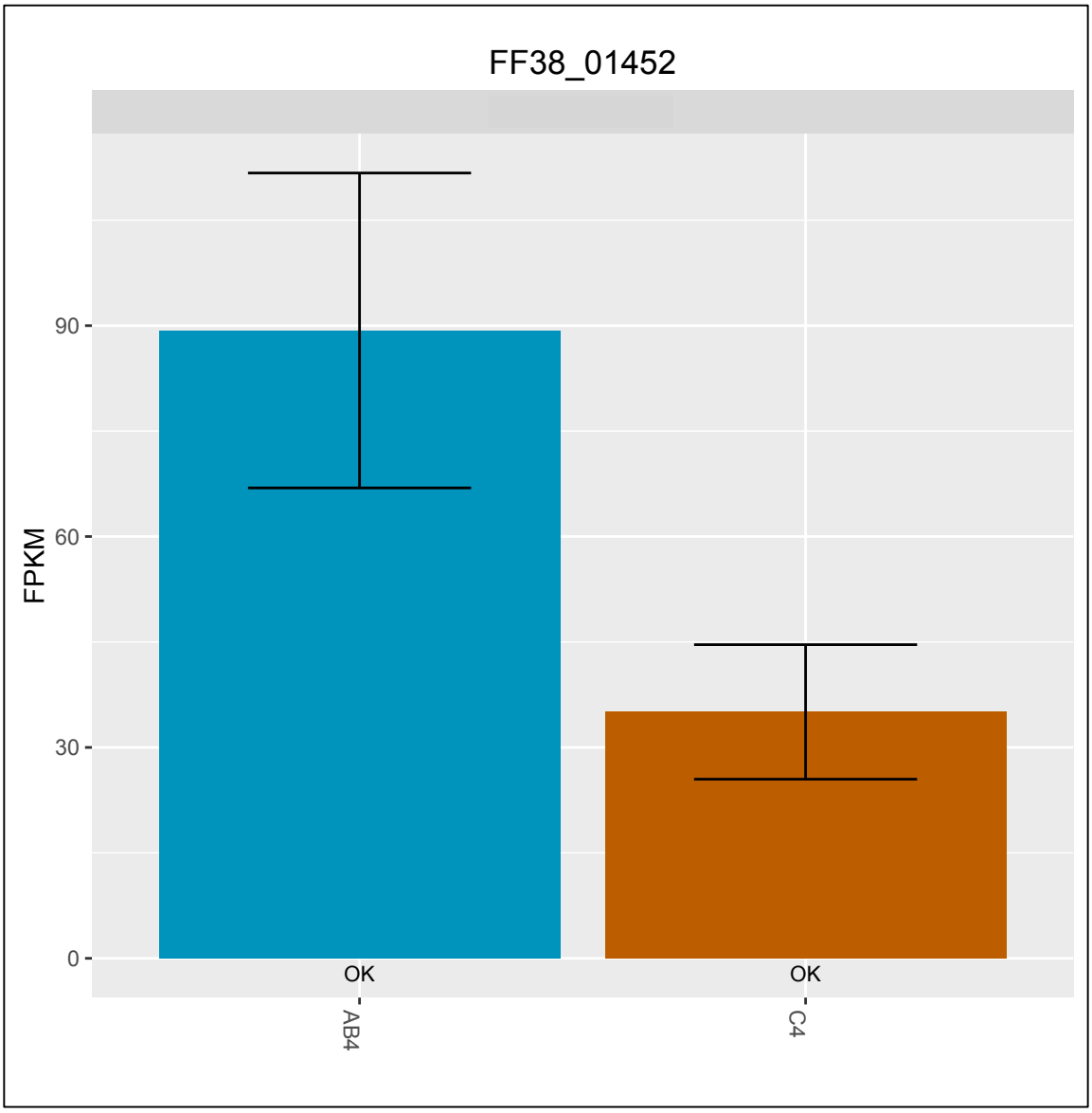

Fig. 8: Barplot displaying expression level fpkm values for gene FF38_01452 (AB4 vs C4). Gene FF38_01452 is associated with a peptidoglycan catabolic process (the chemical reactions and pathways resulting in the breakdown of peptidoglycans, any of a class of glycoconjugates found in bacterial cell walls). FF38_01452 is also up-regulated in PA4 vs C4.

Cuffdiff Analysis with Adjusted TopHat Parameters

Aligning sequencing reads to the *L. cuprina* reference genome using an increased mismatch rate setting in TopHat resulted in an improved alignment rate as compared to using the default settings. In one example, the alignment of sequencing reads to the *L.*

cuprina reference genome resulted in a 48.2.% concordant pair alignment rate when the mismatch and read-edit distance settings were increased to four. Additional TopHat alignment output information from one of the data analysis sets can be seen in Fig. 9.

```
Left reads:
          Input     :  13327997
           Mapped   :   7556944 (56.7% of input)
            of these:    199381 ( 2.6%) have multiple alignments
(121 have >20)
Right reads:
          Input     :  13327997
           Mapped   :   7699612 (57.8% of input)
            of these:    197444 ( 2.6%) have multiple alignments
(122 have >20)
57.2% overall read mapping rate.

Aligned pairs:   6531805
     of these:    166025 ( 2.5%) have multiple alignments
                  104145 ( 1.6%) are discordant alignments
48.2% concordant pair alignment rate.
```

Fig. 9: Example summary of TopHat alignment output with increased mismatch rate and read edit distance parameters.

Analysis of the increased mismatch rate alignment data in Cuffdiff resulted in the identification of several genes that were differentially expressed after larvae were exposed to bacteria.

Table 6 presents a summary of Cuffdiff outputs with adjusted TopHat parameters for AB1 compared to C1. A total of 23 genes displayed significant differential expression ($Q \leq 0.05$) compared to the control when *L sericata* larvae were exposed to *A.baumannii* for 1 h. Five of the 23 differentially expressed genes (22%) were expressed at a higher level in the larvae exposed to *A. baumannii* as compared to the control (ie, upregulated). Relative expression levels of the 23 differentially expressed genes for AB1

vs C1 are displayed in Fig. 10. Gene FF38_08822 (Dmel/edin: defense response to gram negative bacterium) had the greatest fold change for increased gene expression between C1 and AB1. Gene FF38_14463 (uncharacterized protein) had the greatest fold change in terms of decreased gene expression between C1 and AB1.

Table 7 presents a summary of Cuffdiff outputs with adjusted TopHat parameters for PA1 compared to C1. A total of 20 genes displayed significant differential expression ($Q \leq 0.05$) compared to the control when *L sericata* larvae were exposed to *P. aeruginosa* for 1 h. Four of the 20 differentially expressed genes (20%) were expressed at a higher level in the larvae exposed to *P. aeruginosa* as compared to the control (i.e., upregulated). Gene FF38_02709 (uncharacterized protein) had the greatest fold change in terms of increased gene expression between C1 and PA1. Gene FF38_14463 (uncharacterized protein) displayed the greatest fold change for a decrease in gene expression between C1 and PA1.

Table 6 **Summary Table of Cuffdiff Output with Adjusted TopHat Parameters (AB1 vs C1)**

Gene	V1 (AB1)	V2 (C1)	Change[1]	Q value	EL	Gene Description
FF38_08822	4.02319	0.447964	-3.16689	0.01888	Up	Dmel/edin: defense response to gram negative bacterium[4]
FF38_09276	4.69492	1.7115	-1.45584	0.01888	Up	GO:0005549: odorant binding protein[2]
FF38_01916	8.27152	3.73245	-1.14803	0.01888	Up	Dmel/Tweedle (various letters e.g P,N,O,B…): structural constituent of chitin based cuticle[4]
FF38_04326	4.35223	1.59031	-1.45244	0.01888	Up	Dmel/pirk Poor Imd response upon knock-in is a negative regulator of the Immune Deficiency (Imd) pathway, acting at the level of PGRP-LC. Being regulated by the Imd pathway itself, it establishes a negative feedback loop adjusting Imd pathway activity to the severity of infection[4]
FF38_09383	2.3459	0.501464	-2.22593	0.01888	Up	Attacin-A, GO:0005576: extracellular region, Attacin_N and Attacin_C (antimicrobial peptides)[2]
FF38_02450	21.5458	43.8889	1.02645	0.01888	Down	GO:0042302: structural constituent of cuticle[2]
FF38_06150	9.01248	17.127	0.926279	0.0492522	Down	GO:0008152: metabolic process, catalytic/alkaline phosphatase activity[2]
FF38_14459	3.07672	32.4358	3.39812	0.01888	Down	Protein coding[3]
FF38_14463	0.311916	7.31653	4.55193	0.01888	Down	Protein coding[3]
FF38_14461	0	0.642927	inf	0.01888	Down	Protein coding[3]
FF38_14458	1.15995	8.00718	2.78724	0.01888	Down	Protein coding[3]
FF38_14465	0.583781	8.58746	3.87873	0.01888	Down	Protein coding[3]
FF38_04943	1.31274	3.65499	1.47729	0.01888	Down	GO:0006810: intracellular transport[2]

Table 6 Continued

Gene	V1 (AB1)	V2 (C1)	Change [1]	Q value	EL	Gene Description
FF38_12518	3.15021	7.64388	1.27886	0.01888	Down	GO:0016021: integral component of plasma membrane[2]; also, Dmel/Osiris2 [4]
FF38_12526	0.328513	0.986172	1.58589	0.0359619	Down	GO:0016021: integral component of plasma membrane[2], also Dmel/Osiris9[4]
FF38_12536	0.381483	5.9404	3.96087	0.01888	Down	Dmel/Osiris15: inferred integral component of plasma membrane[4]
FF38_06986	0.0782144	0.547015	2.80607	0.01888	Down	Protein coding[3]
FF38_02323	0.413629	1.58955	1.94221	0.01888	Down	Dmel/Spt7: contributes to histone acetyltransferase activity, SAGA complex[4]
FF38_02738	5.60945	19.152	1.77156	0.01888	Down	Protein coding[3]
FF38_02650	16.1981	38.8724	1.26293	0.01888	Down	GO:0004867: serine-type endopeptidase inhibitor activity[2]
FF38_03322	1.75844	4.66705	1.40821	0.0492522	Down	Protein coding[3]
FF38_07366	0.879774	1.77354	1.01143	0.01888	Down	GO:0004867: serine-type endopeptidase inhibitor activity[2]
FF38_00565	2.63618	5.77256	1.13076	0.01888	Down	Protein coding[3]

Abbreviations: PA4 = larvae exposed to *A. baumannii* for 1 h, C1 = control group larvae not exposed to bacteria for 1 h, EL = expression level, GO = Gene ontology GO term, V1 = Value 1, V2 = Value 2.

Note: Significant values defined as $Q \leq 0.05$.

[1] Change presented as log 2 (fold change) function.

Source: [2] InterPro via EnsemblMetazoa, [3] EnsemblMetazoa, [4] FlyBase.

Table 7 Summary Table of Cuffdiff Output with Adjusted TopHat Parameters (PA1 vs C1)

Gene	V1 (PA1)	V2 (C1)	Change[1]	Q value	EL	Gene Description
FF38_02709	7.20823	2.45667	-1.55294	0.0294115	Up	Protein coding[3]
FF38_01916	9.66887	3.83516	-1.33406	0.0294115	Up	Dmel/Tweedle: structural constituent of chitin based cuticle[4]
FF38_05420	6.6478	3.1884	-1.06004	0.038235	Up	GO 0016021: integral component of membrane[2]
FF38_01455	45.357	22.4764	-1.01292	0.038235	Up	Protein coding[3]
FF38_02450	22.8271	44.9909	0.978885	0.0294115	Down	GO:0042302: structural constituent of cuticle[2]
FF38_10331	24.5678	53.989	1.1359	0.038235	Down	Dmel/Gnmt: FBgn0038074 [4]; GO:0017174: Glycine N-Methyltransferase activity[2]
FF38_12518	3.52907	7.8344	1.15053	0.038235	Down	GO:0016021: integral component of membrane[2]
FF38_03845	1.18485	2.74636	1.21281	0.0294115	Down	GO:0007264: Rad and Gem related GTP binding protein 1, small GTPase mediated signal transduction[2]
FF38_03381	30.8557	72.7032	1.23648	0.0294115	Down	GO:0006030: chitin metabolic process, chitin binding[2], also Dmel/Peritrophin-15a/15b[4]
FF38_02650	15.5385	39.8184	1.35759	0.0294115	Down	GO:0004867: serine-type endopeptidase inhibitor activity[2]; PTHR10083:SF192: immune system process[5]
FF38_02738	7.39233	19.6362	1.40942	0.0294115	Down	Protein coding
FF38_04943	1.37335	3.7474	1.44819	0.038235	Down	PTHR23324: transfer/carrier protein transporter[5]
FF38_04030	3.78797	11.4848	1.60023	0.0294115	Down	PTHR22762: glucosidase[5]
FF38_12526	0.319991	1.01039	1.6588	0.038235	Down	Protein coding[3]
FF38_03322	1.37683	4.78086	1.79592	0.038235	Down	Protein coding[3]
FF38_06986	0.0944128	0.560499	2.56966	0.0294115	Down	PTHR11559: hydrolase, esterase[5]; lipase in Dmel[4]
FF38_14465	1.38616	8.78805	2.66445	0.0294115	Down	Protein coding[3]

Table 7 Continued

Gene	V1 (PA1)	V2 (C1)	Change[1]	Q value	EL	Gene Description
FF38_03319	1.64816	11.8379	2.84448	0.0294115	Down	Protein coding[3]
FF38_12536	0.302546	6.07935	4.32869	0.0294115	Down	Dmel/Osiris15: inferred: integral component of plasma membrane[4]
FF38_14463	0.223132	7.48631	5.06829	0.0294115	Down	Protein coding[3]

Abbreviations: PA1 = larvae exposed to *P. aeruginosa* for 1 h, C1 = control group larvae not exposed to bacteria for 1 h, EL = expression level, GO = Gene ontology GO term, V1 = Value 1, V2 = Value 2.

Note: Significant values defined as $Q \leq 0.05$.

[1] Change presented as log 2 (fold change) function.

Source: [2] InterPro via EnsemblMetazoa, [3] EnsemblMetazoa, [4] FlyBase,[5] Panther GO Terms

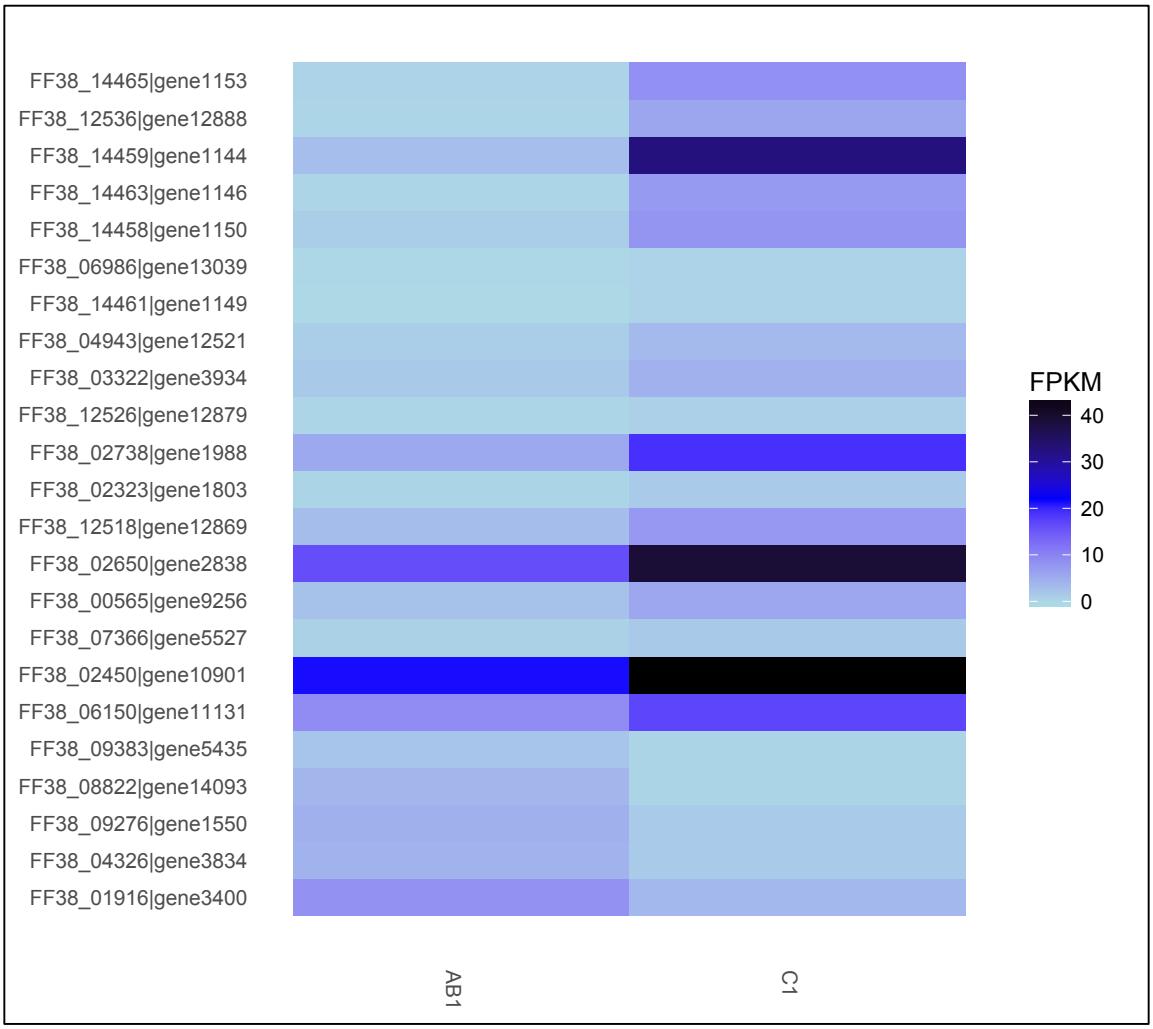

Fig. 10: Heatmap displaying relative expression levels of genes that are differentially expressed between larvae exposed to *A. baumannii* for one hour (AB1) and control group larvae (C1). Expression levels between samples are compared in terms of normalized mapped read (FPKM) values. Light blue coloring corresponds to lower levels of gene expression and black coloring corresponds to higher levels of gene expression.

Pairwise comparisons of expression levels for all genes from Cuffdiff output is presented in Fig. 11 (AB1 vs C1) as well as in Fig. 12 (PA1 vs C1).

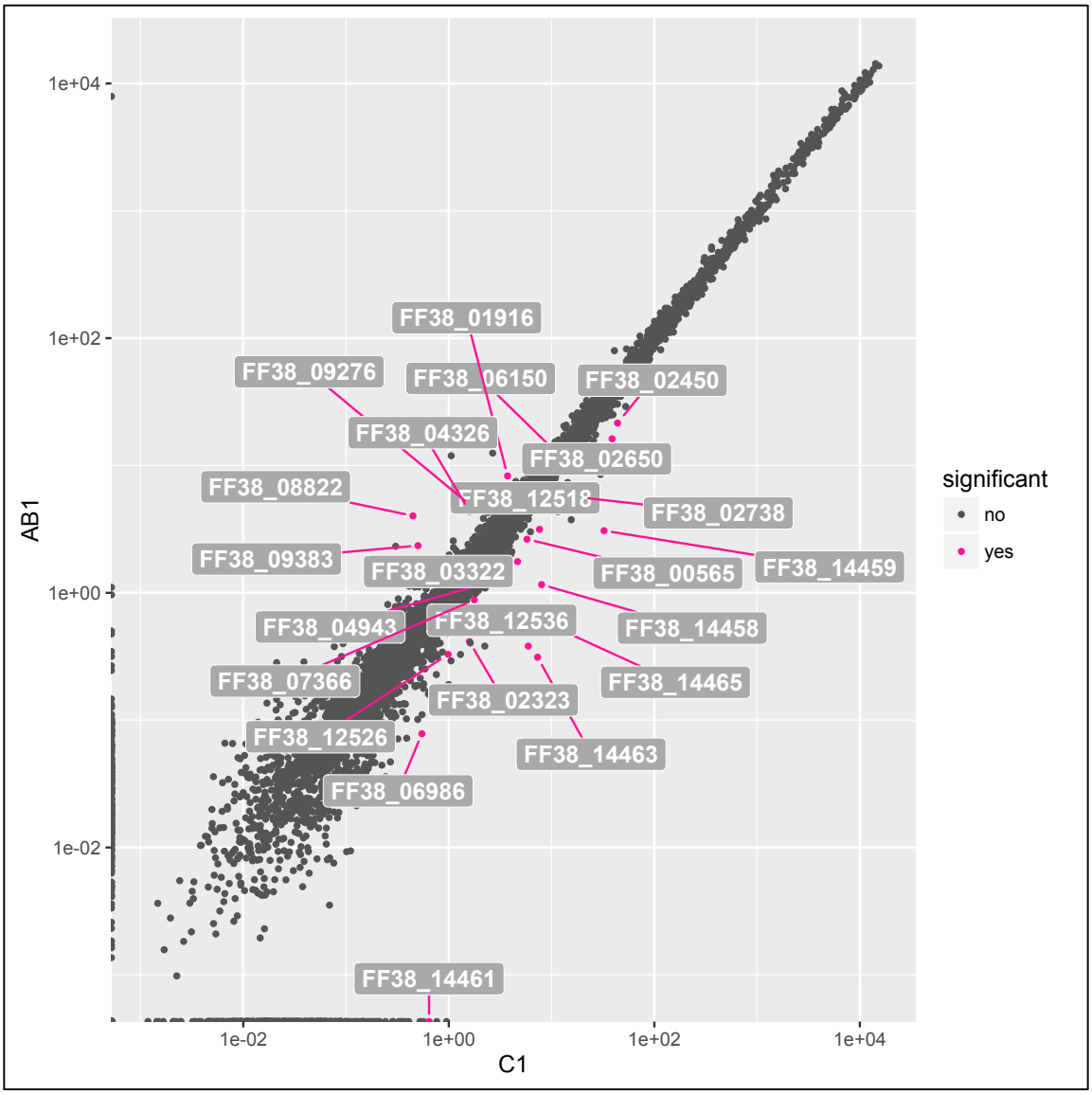

Fig. 11: Scatterplot of pairwise gene expression levels between AB1 and C1 with log10 transformed FPKM values. Genes that are differentially expressed at a significant level are highlighted and labeled. A data point above y=x represents a gene that is expressed at higher level in AB1 than in C1.

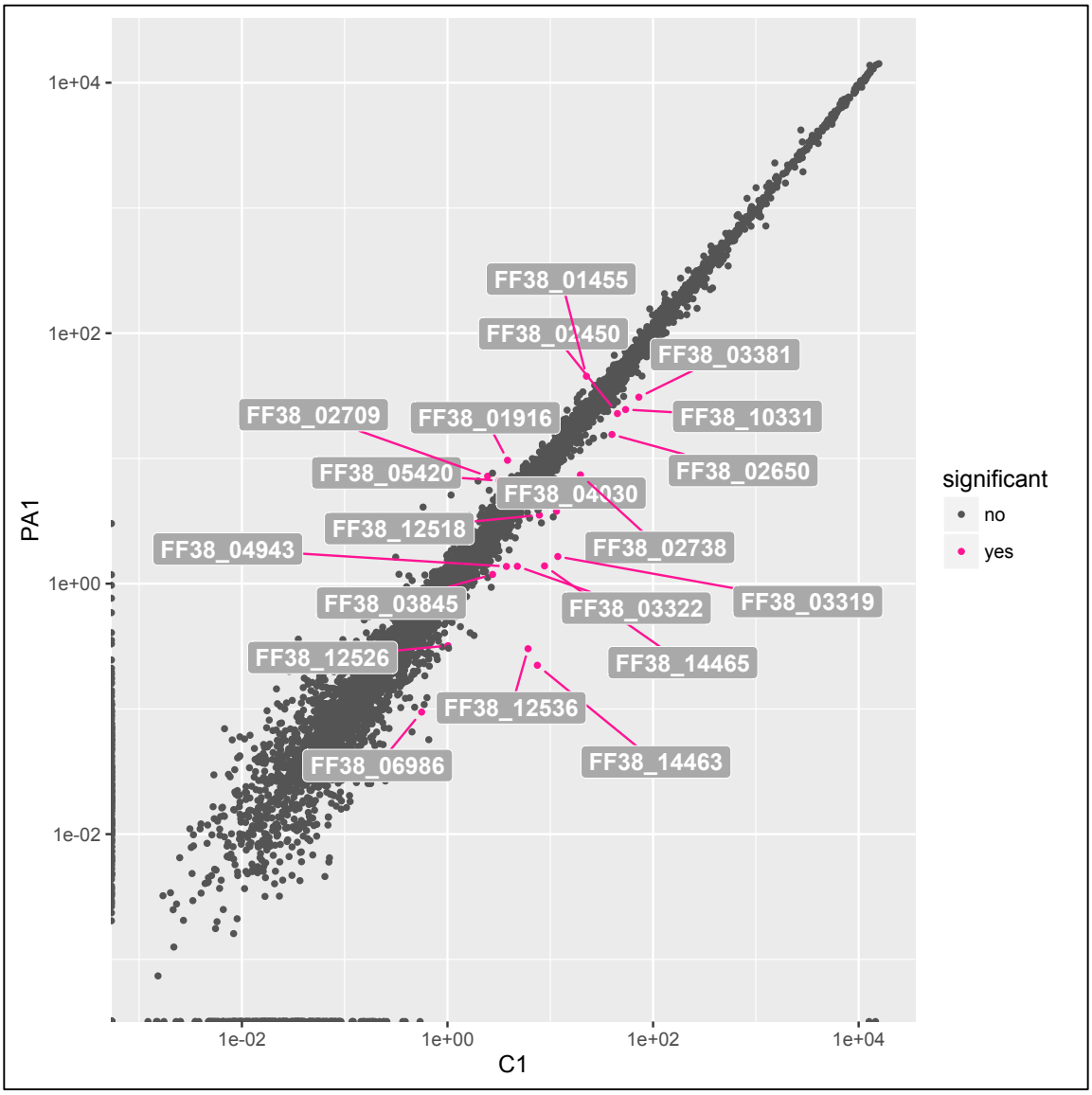

Fig. 12: Scatterplot of pairwise gene expression levels between PA1 and C1 with log10 transformed FPKM values. Genes that are differentially expressed at a significant level are highlighted and labeled. A data point above y=x represents a gene that is expressed at higher level in PA1 than in C1.

Table 8 presents a summary of Cuffdiff outputs with adjusted TopHat parameters for AB4 compared to C4. A total of 55 genes displayed significant differential expression ($Q \leq 0.05$) compared to the control when *L. sericata* larvae were exposed to *A. baumannii* for 4 h. Thirty-nine of the 55 differentially expressed genes (71%) were

expressed at a higher level in the larvae exposed to *A. baumannii* as compared to the control (i.e., upregulated). Gene FF38_00375 (endopeptidase inhibitor activity) had the greatest fold change for increased gene expression between C4 and AB4. Gene FF38_14458 (uncharacterized protein) had the greatest fold change in terms of decreased gene expression between C4 and AB4.

Table 9 presents a summary of Cuffdiff outputs with adjusted TopHat parameters for PA4 compared to C4. A total of 21 genes displayed significant differential expression ($Q \leq 0.05$) compared to the control when *L sericata* larvae were exposed to *P aeruginosa* for 4 h. Eleven of the 21 differentially expressed genes (52%) were expressed at a higher level in the larvae exposed to *P. aeruginosa* as compared to the control (ie, upregulated). Gene FF38_05988 (Dmel\Hsp22: Heat shock protein) had the greatest fold change for increased gene expression between C4 and PA4. Genes FF38_14459 and FF38_00716 (uncharacterized proteins) had the greatest fold changes in terms of decreased gene expression between C4 and PA4.

Table 8 **Summary Table of Cuffdiff Output with Adjusted TopHat Parameters (AB4 vs C4)**

Gene	V1 (AB4)	V2 (C4)	Change[1]	Q value	EL	Gene Description
FF38_00041	1.54674	0.776243	-0.994649	0.0495804	Up	Zinc finger protein-related (PTHR22979)[5]
FF38_00375	1.08192	0.136901	-2.98239	0.0115688	Up	GO:0004866; endopeptidase inhibitor activity, Alpha-2-macroglobulin[2], also Dmel/Tep1 + 2: Thioester-containing protein 1 + 2 [4]
FF38_00565	4.46969	2.7702	-0.690183	0.0115688	Up	Protein coding[3]
FF38_01073	8.12816	4.42301	-0.8779	0.0115688	Up	GO:0005515: Interacting selectively and non-covalently with any protein or protein complex (a complex of two or more proteins that may include other non-protein molecules)[2]; Dmel/ecd ecdysoneless[4]
FF38_01326	6.27991	4.16833	-0.591274	0.0115688	Up	GO:0019752: carboxylic acid metabolic process, GO:0006520: cellular amino acid metabolic process[2]
FF38_01452	113.376	48.0906	-1.23729	0.0115688	Up	GO:0008745: N-acetylmuramoyl-L-alanine amidase activity - proteins containing this domain include zinc amidases that have N-acetylmuramoyl-L-alanine amidase activity EC:3.5.1.28. This enzyme domain cleaves the amide bond between N-acetylmuramoyl and L-amino acids in bacterial cell walls (preferentially: D-lactyl-L-Ala)[2], GO:0008270; zinc ion binding, Peptidoglycan-recognition protein SB1[2]
FF38_01558	1.0339	0.56844	-0.863014	0.0115688	Up	GO:0005515: protein binding, Immunoglobulin-like domain[2]
FF38_02341	0.593508	0.353284	-0.74844	0.0115688	Up	Cytokine receptor[3], Ig-like domain and FN3 domain[2]
FF38_02450	12.6222	8.30891	-0.603233	0.031092	Up	GO:0042302: structural constituent of cuticle[2]
FF38_02573	15.1712	10.166	-0.577592	0.0114309	Up	Protein coding[3]
FF38_02624	563.525	215.177	-1.38895	0.031092	Up	Protein coding[3]
FF38_02631	103.538	41.3612	-1.32381	0.0114309	Up	Protein coding[3]

Table 8 Continued

Gene	V1 (AB4)	V2 (C4)	Change[1]	Q value	EL	Gene Description
FF38_02640	7.17193	3.52667	-1.02405	0.0253467	Up	GO:0055114: oxidation-reduction process, TauD/TfdA-like domain[2]
FF38_02650	15.4517	8.54324	-0.854912	0.0114309	Up	GO:0004867: serine-type endopeptidase inhibitor activity[2]
FF38_03041	3.1772	1.77464	-0.84023	0.0114309	Up	GO:0005515: protein binding, Immunoglobulin-like domain[2]
FF38_03845	2.2137	1.14499	-0.951129	0.0114309	Up	GO:0007264: Rad and Gem related GTP binding protein 1; small GTPase mediated signal transduction[2]
FF38_04236	0.835452	0.249738	-1.74214	0.0114309	Up	GO:0006508: proteolysis, Cathepsin L[2]
FF38_04326	5.63907	3.24967	-0.795163	0.0114309	Up	Dmel/pirk Poor Imd response upon knock-in is a negative regulator of the Immune Deficiency (Imd) pathway, acting at the level of PGRP-LC. Being regulated by the Imd pathway itself, it establishes a negative feedback loop adjusting Imd pathway activity to the severity of infection[4]
FF38_04937	0.441045	0.209709	-1.07254	0.0114309	Up	GO:0004252: serine-type endopeptidase activity, Serine protease easter[2]
FF38_04966	7.2273	4.54245	-0.669987	0.0114309	Up	GO:0006508: proteolysis, serine protease snake, Peptidase S1A, chymotrypsin family[2]
FF38_05096	1333.82	905.746	-0.558391	0.0114309	Up	GO:0042302: structural constituent of cuticle[2]
FF38_05499	523.276	248.648	-1.07347	0.0381029	Up	Protein coding[3]
FF38_06150	3.26257	1.66263	-0.972545	0.0114309	Up	GO:0008152: metabolic process, catalytic/alkaline phosphatase activity[2]
FF38_06209	0.396645	0.158991	-1.3189	0.0114309	Up	GO:0006836: neurotransmitter transport[2]
FF38_06525	11.7206	8.02734	-0.546048	0.0114309	Up	GO:0055114: oxidation-reduction process, GO:0016491: oxidoreductase activity[2]; TauD/TfdA-like domain[2]

Table 8 Continued

Gene	V1 (AB4)	V2 (C4)	Change[1]	Q value	EL	Gene Description
FF38_06989	50.0383	30.8677	-0.696933	0.0199308	Up	Protein coding[3]
FF38_07255	43.5559	30.3178	-0.522703	0.0253467	Up	Titin, GO:0005515; protein binding, Ig-like domains are involved in a variety of functions, including cell-cell recognition, cell-surface receptors, muscle structure and the immune system[2], SH3 domain, Fibronectin type III, N3 exhibits functional as well as structural modularity[2]. Sites of interaction with other molecules have been mapped to short stretch of amino acids such as the Arg-Gly-Asp (RGD) sequence found in various FN3 domains[2]. The RGD sequences are involved in interactions with integrin[2]. Small peptides containing the RGD sequence can modulate a variety of cell adhesion invents associated with thrombosis, inflammation, and tumor metastasis[2]. These properties have led to the investigation of RGD peptides and RGD peptide analogs as potential therapeutic agents[2]
FF38_07308	14.2416	7.65268	-0.896074	0.031092	Up	GO:0003676; nucleic acid binding, GO:0008270; zinc ion binding, GO:0046872; metal ion binding, Zinc finger C2H2-type/integrase DNA-binding domain[2]
FF38_07373	7.29176	4.20396	-0.794518	0.0199308	Up	GO:0055114; oxidation-reduction process, putative cytochrome P450 6g2 [2]
FF38_08124	44.853	28.4741	-0.655552	0.0114309	Up	GO:0005576: extracellular region; transferrin like domain; Transferrins are a family of eukaryotic iron-binding glycoproteins that share the common function of controlling the level of free iron in biological fluids[2]
FF38_08822	4.4567	1.37675	-1.69471	0.0114309	Up	Dmel/edin: defense response to gram negative bacterium[4]

Table 8 Continued

Gene	V1 (AB4)	V2 (C4)	Change[1]	Q value	EL	Gene Description
FF38_09276	3.55035	1.21834	-1.54305	0.0114309	Up	GO:0005549: odorant binding protein[2]
FF38_10256	1.1468	0.722912	-0.665719	0.0431833	Up	Protein coding[3]
FF38_10586	1.0609	0.455742	-1.219	0.0114309	Up	GO:0035556: Intracellular signal transduction, GO:0046872: metal ion binding, GO:0005622: Intracellular; Protein kinase C-like, phorbol ester/diacylglycerol-binding domain[2]
FF38_11848	23.7023	13.1249	-0.852727	0.0253467	Up	Protein coding[3]
FF38_12829	4.29603	2.07703	-1.04848	0.0114309	Up	GO:0008152: metabolic process, GO:0003824: catalytic activity [Source:Ensembl] GO:008152; metabolic process; catalytic activity; AMP-dependent synthetase/ligase[2]
FF38_13318	3.52794	2.34059	-0.591951	0.0114309	Up	Broad-complex core protein isoforms 1/2/3/4/5 [3], BTB/POZ_dom[2]
FF38_14361	4.29547	2.37229	-0.856537	0.0114309	Up	GO:0006355: DNA-binding protein D-ETS-6[2], GO:0003700: transcription factor activity, sequence-specific DNA binding[2]
FF38_14544	2.57945	1.72996	-0.576326	0.0114309	Up	GO:0005515: protein binding. Immunoglobulin-like domain[2]
FF38_00744	19.1241	27.2191	0.509227	0.0114309	Down	GO:0008061: chitin binding, GO:0005576: extracellular region, GO:0006030: chitin metabolic process[2]
FF38_01660	245.345	370.152	0.59331	0.0114309	Down	GYR motif: Its function is unknown; however, the presence of completely conserved tyrosine residues may suggest it could be a substrate for tyrosine kinases[2]
FF38_01932	9.94015	14.5867	0.553315	0.0114309	Down	GO:0042302; structural constituent of cuticle[2]
FF38_02709	5.33025	16.5788	1.63707	0.0114309	Down	Protein coding[3]
FF38_04030	0.887258	1.60498	0.855129	0.0114309	Down	GO:0004553; hydrolase activity, hydrolyzing O-glycosyl compounds[2]

Table 8 Continued

Gene	V1 (AB4)	V2 (C4)	Change[1]	Q value	EL	Gene Description
FF38_04791	33.9035	59.9869	0.823212	0.031092	Down	Protein coding[3]
FF38_05172	29.9994	57.2836	0.933189	0.0114309	Down	Protein coding[3]
FF38_08169	6.55904	12.26	0.902399	0.0114309	Down	Protein coding[3]
FF38_09115	1.81841	3.68342	1.01837	0.0431833	Down	Protein binding[3]
FF38_09596	149.798	238.559	0.671329	0.0253467	Down	GO:0003796: lysozyme activity[2]
FF38_12201	50.4258	75.5139	0.582581	0.0494645	Down	Protein coding[3]
FF38_12202	115.576	170.843	0.563837	0.0114309	Down	Protein coding[3]
FF38_13360	1.51754	2.43457	0.681937	0.0253467	Down	GO:0080019: fatty-acyl-CoA reductase (alcohol-forming) activity[2]
FF38_14458	1.24446	4.5172	1.85991	0.0114309	Down	Protein coding[3]
FF38_14459	10.1282	30.0593	1.56943	0.0114309	Down	Protein coding[3]
FF38_14466	1.59405	3.08638	0.953225	0.0114309	Down	Protein coding[3]

Abbreviations: AB4 = larvae exposed to *A.* baumannii for 4 h, C4 = control group larvae not exposed to bacteria for 4 h, EL = expression level, GO = Gene ontology GO term, V1 = Value 1, V2 = Value 2.

Note: Significant values defined as $Q \leq 0.05$.

[1] Change presented as log 2 (fold change) function.

Source: [2] InterPro via EnsemblMetazoa, [3] EnsemblMetazoa, [4] FlyBase, [5] Panther GO Terms

Table 9 Summary Table of Cuffdiff Output with Adjusted TopHat Parameters (PA4 vs C4)

Gene	V1 (PA1)	V2 (C1)	Change[1]	Q value	EL	Gene Description
FF38_05988	6.37032	1.04205	-2.61194	0.0213056	Up	Dmel\Hsp22: Heat shock protein[4]; Alpha-crystallin/Heat shock protein: Alpha-crystallin has chaperone-like properties including the ability to prevent the precipitation of denatured proteins and to increase cellular tolerance to stress[2]
FF38_04236	0.84037	0.241859	-1.79686	0.0213056	Up	GO:0006508, proteolysis, Cathepsin L[2]
FF38_08822	3.64648	1.32953	-1.45559	0.0213056	Up	Dmel/edin: defense response to gram negative bacterium[4]
FF38_09514	9.28661	3.78323	-1.29553	0.0213056	Up	GO:0005515: Kazal domain, serine proteinase inhibitors[2]
FF38_01452	100.507	46.5364	-1.11087	0.0213056	Up	GO:0008745: N-acetylmuramoyl-L-alanine amidase activity,Proteins containing this domain include zinc amidases that have N-acetylmuramoyl-L-alanine amidase activity EC:3.5.1.28. This enzyme domain cleaves the amide bond between N-acetylmuramoyl and L-amino acids in bacterial cell walls (preferentially: D-lactyl-L-Ala), GO:0008270: zinc ion binding, Peptidoglycan-recognition protein SB1 [2]
FF38_10026	1.83936	0.936239	-0.974259	0.0213056	Up	GO:0016021; transferase activity, transferring acyl groups other than amino-acyl groups[2]
FF38_04326	5.74375	3.14782	-0.867639	0.0365238	Up	Dmel/pirk: Poor Imd response upon knock-in is a negative regulator of the Immune Deficiency (Imd) pathway, acting at the level of PGRP-LC. Being regulated by the Imd pathway itself, it establishes a negative feedback loop adjusting Imd pathway activity to the severity of infection[4]
FF38_08298	1.38783	0.819951	-0.759221	0.0213056	Up	Dmel\CG8492: protein coding[4]; Glycoside hydrolase family 22, Lysozome like domain[2]

Table 9 Continued

Gene	V1 (PA1)	V2 (C1)	Change[1]	Q value	EL	Gene Description
FF38_07809	29.3975	17.7661	-0.726568	0.0213056	Up	Dmel\Lst Limostatin: Limostatin (Lst) is a peptide hormone produced by endocrine corpora cardiaca cells during starvation. Lst suppresses insulin production and secretion from insulin-producing cells by signaling through the G-protein coupled receptor PK1-R[4]
FF38_05096	1349.58	876.674	-0.622398	0.0213056	Up	GO:0042302: structural constituent of cuticle[2]
FF38_06525	11.9178	7.78031	-0.61522	0.0365238	Up	GO:0055114: oxidation-reduction process, GO:0016491: oxidoreductase activity, TauD/TfdA-like domain[2]
FF38_01660	234.51	358.503	0.612334	0.0213056	Down	GYR motif: Its function is unknown, however the presence of completely conserved tyrosine residues may suggest it could be a substrate for tyrosine kinases[2]
FF38_08047	2.05813	3.50193	0.766816	0.0365238	Down	GO:0004222: metalloendopeptidase activity involved in the catalysis of the hydrolysis of internal, alpha-peptide bonds in a polypeptide chain[2]; GO:0008270: zinc ion binding defined as interacting selectively and non-covalently with zinc (Zn) ions[2]
FF38_06814	2.29002	4.18812	0.87094	0.0213056	Down	GO:0004252: serine-type endopeptidase activity[2]
FF38_02709	6.96294	16.1045	1.2097	0.0213056	Down	Protein coding[3]
FF38_14466	1.04929	2.99551	1.51339	0.0213056	Down	Protein coding[3]
FF38_02631	10.8862	40.0823	1.88047	0.0213056	Down	Protein coding[3]
FF38_02624	53.8452	208.54	1.95343	0.0213056	Down	Protein coding[3]
FF38_14458	0.834344	4.38123	2.39262	0.0213056	Down	Protein coding[3]
FF38_14459	2.68447	29.1856	3.44255	0.0213056	Down	Protein coding[3]
FF38_00716	0	11.6449	inf	0.0213056	Down	Protein coding[3]

Table 9 Continued

Gene	V1 (PA1)	V2 (C1)	Change[1]	Q value	EL	Gene Description

Abbreviations: PA4 = larvae exposed to *P. aeruginosa* for 4 h, C4 = control group larvae not exposed to bacteria for 4 h, EL = expression level, GO = Gene ontology GO term, V1 = Value 1, V2 = Value 2.

Note: Significant values defined as $Q \leq 0.05$.

[1] Change presented as log 2 (fold change) function.

Source: [2] InterPro via EnsemblMetazoa, [3] EnsemblMetazoa, [4] FlyBase.

Pairwise comparisons of expression levels for all genes from Cuffdiff output are presented in Fig. 13 (AB4 vs C4) as well as in Fig. 14 (PA4 vs C4).

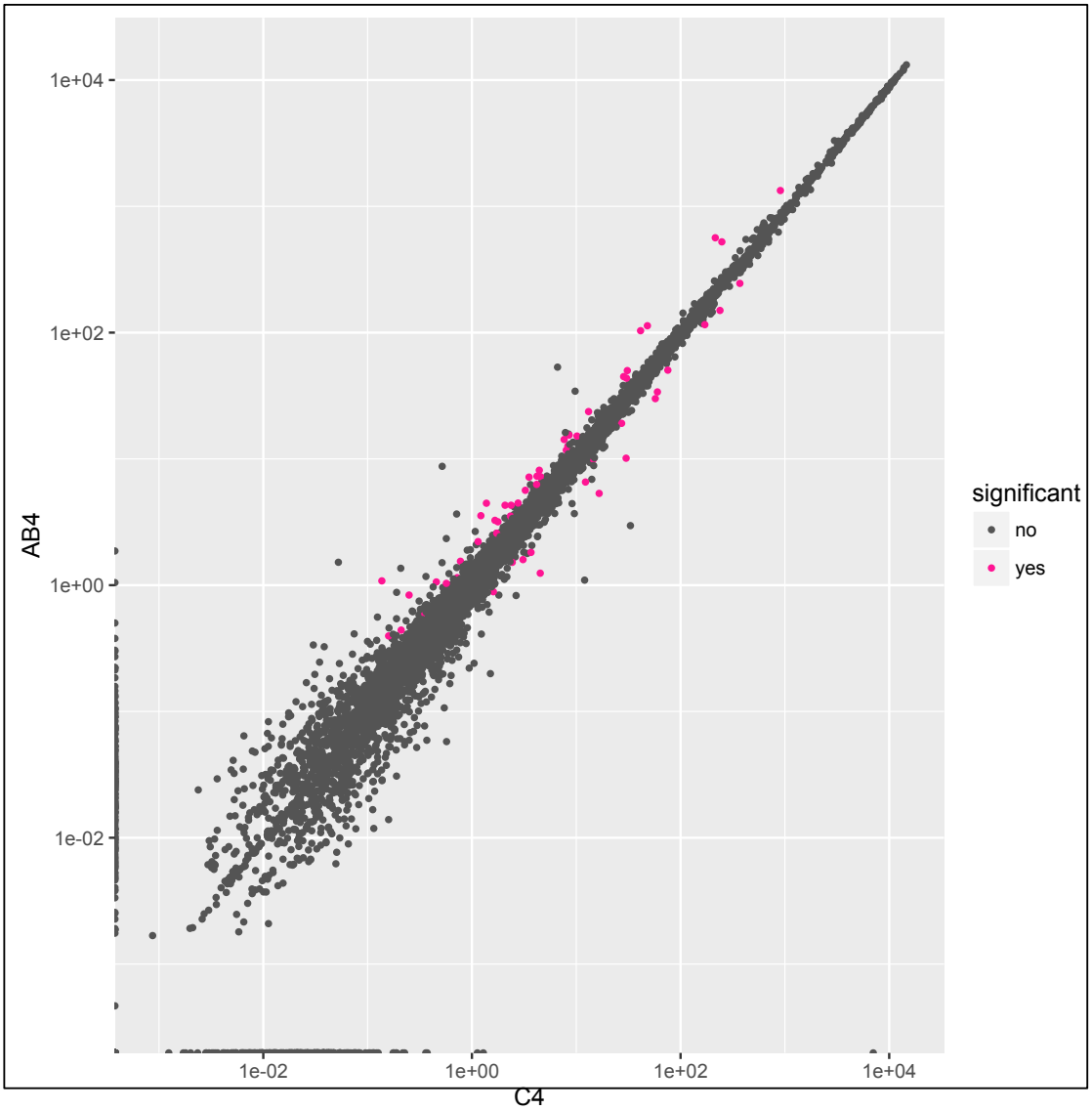

Fig. 13: Scatterplot of pairwise gene expression levels between AB4 and C4 with log10 transformed FPKM values. Genes that are differentially expressed at a significant level are colored pink. A data point above y=x represents a gene that is expressed at higher level in AB4 than in C4.

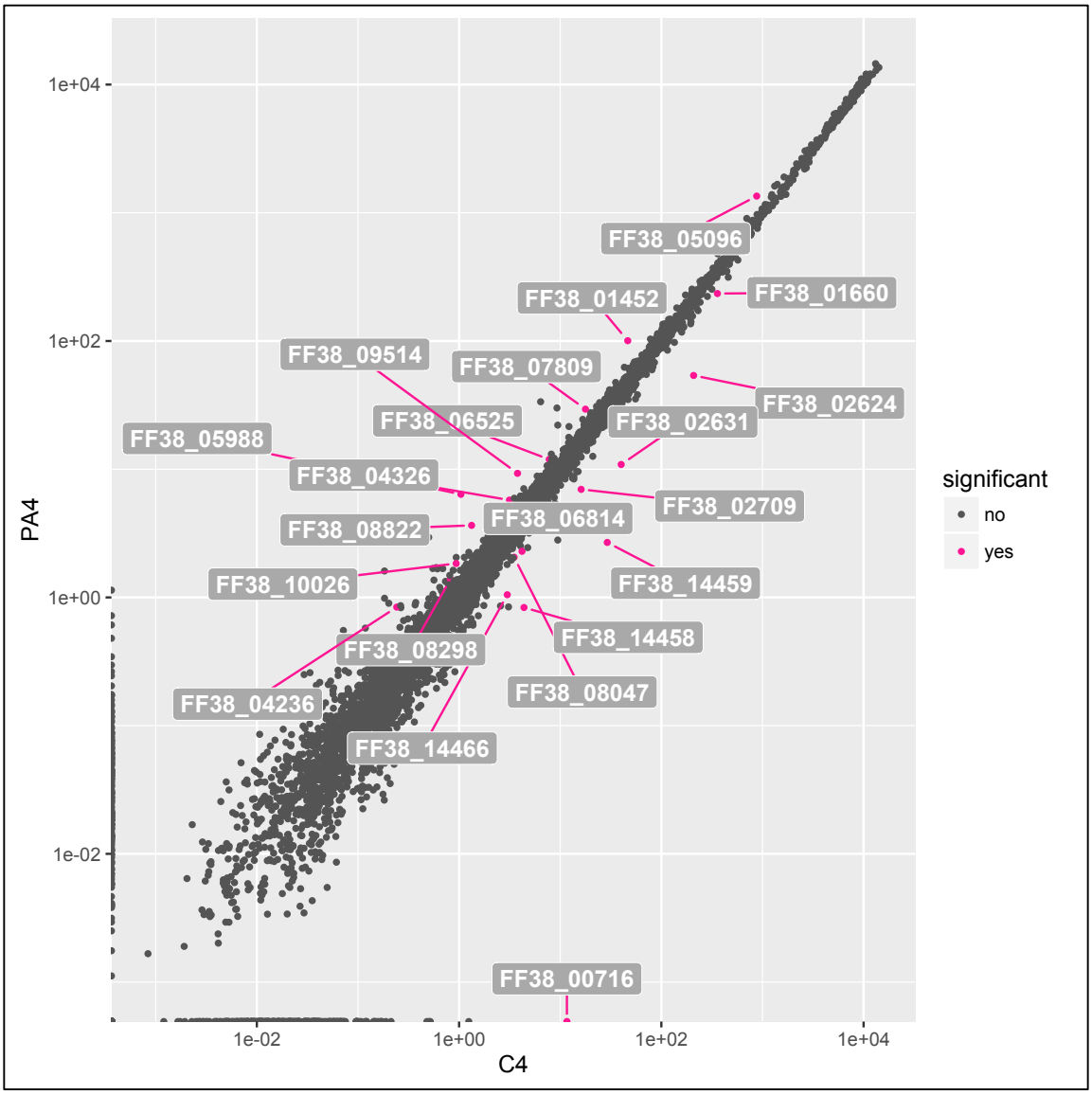

Fig. 14: Scatterplot of pairwise gene expression levels between PA4 and C4 with log10 transformed FPKM values. Genes that are differentially expressed at a significant level are highlighted and labeled. A data point above y=x represents a gene that is expressed at higher level in PA4 than in C4.

Seventeen down-regulated differentially expressed genes were common to more than one analysis set; the Venn diagram in Fig. 15 presents the down-regulated significant differentially expressed genes as they appear in each Cuffdiff analysis performed with adjusted TopHat parameters. Eleven down-regulated genes are present in

both the AB1 vs C1 and PA1 vs C1 data sets. Genes FF38_01660 (possible substrate for tyrosine kinase), FF38_02709 (uncharacterized protein), and FF38_14466 (uncharacterized protein) were down-regulated in both AB4 vs C4 and PA4 vs C4. Genes FF38_14458 (uncharacterized protein) and FF38_14459 (uncharacterized protein) were found to be down-regulated in AB1 vs C1, AB4 vs C4, and PA4 vs C4. Gene FF38_04030 (hydrolase activity, hydrolyzing O-glycosyl compounds) was down-regulated in AB4 vs C4 and PA1 vs C1. No down-regulated genes were represented in all four of the analysis sets.

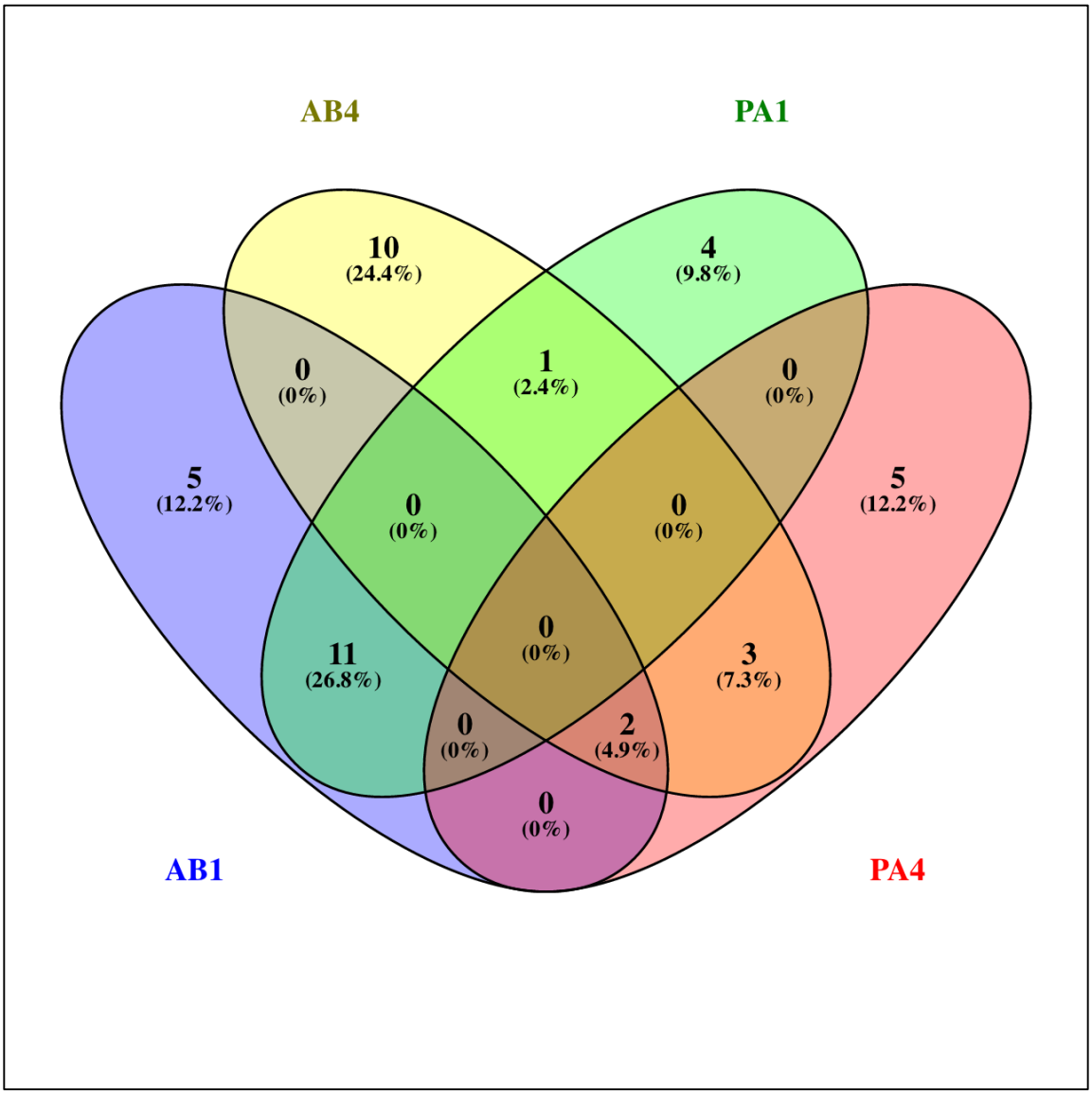

Fig. 15: Four-way Venn diagram displaying overlapping counts of significant differentially expressed genes that are down-regulated.

The up-regulated genes displaying significant differential expression from all Cuffdiff analysis sets are presented in the Venn diagram in Fig. 16. Gene FF38_01916 (structural constituent of chitin based cuticle) was found to be up-regulated in both AB1 vs C1 and PA1 vs C1. Gene FF38_09276 (odorant binding protein) was up-regulated in both AB1 vs C1 and AB4 vs C4. Genes FF38_01452 (peptidoglycan catabolic process),

FF38_04236 (proteolysis), FF38_05096 (structural constituent of cuticle), and FF38_06525 (oxido-reductase activity) were up-regulated in AB4 vs C4 and PA4 vs C4. Genes FF38_08822 (Dmel/edin: defense response to gram negative bacterium) and FF38_04326 (a negative regulator of the Immune Deficiency (Imd) pathway) were up-regulated in AB1 vs C1, AB4 vs C4, and PA4 vs C4. No up-regulated genes were represented in all four of the analysis sets. Expression levels for gene FF38_01452, which is also up-regulated in AB4 and PA4 with default TopHat parameters, are displayed in Fig. 17.

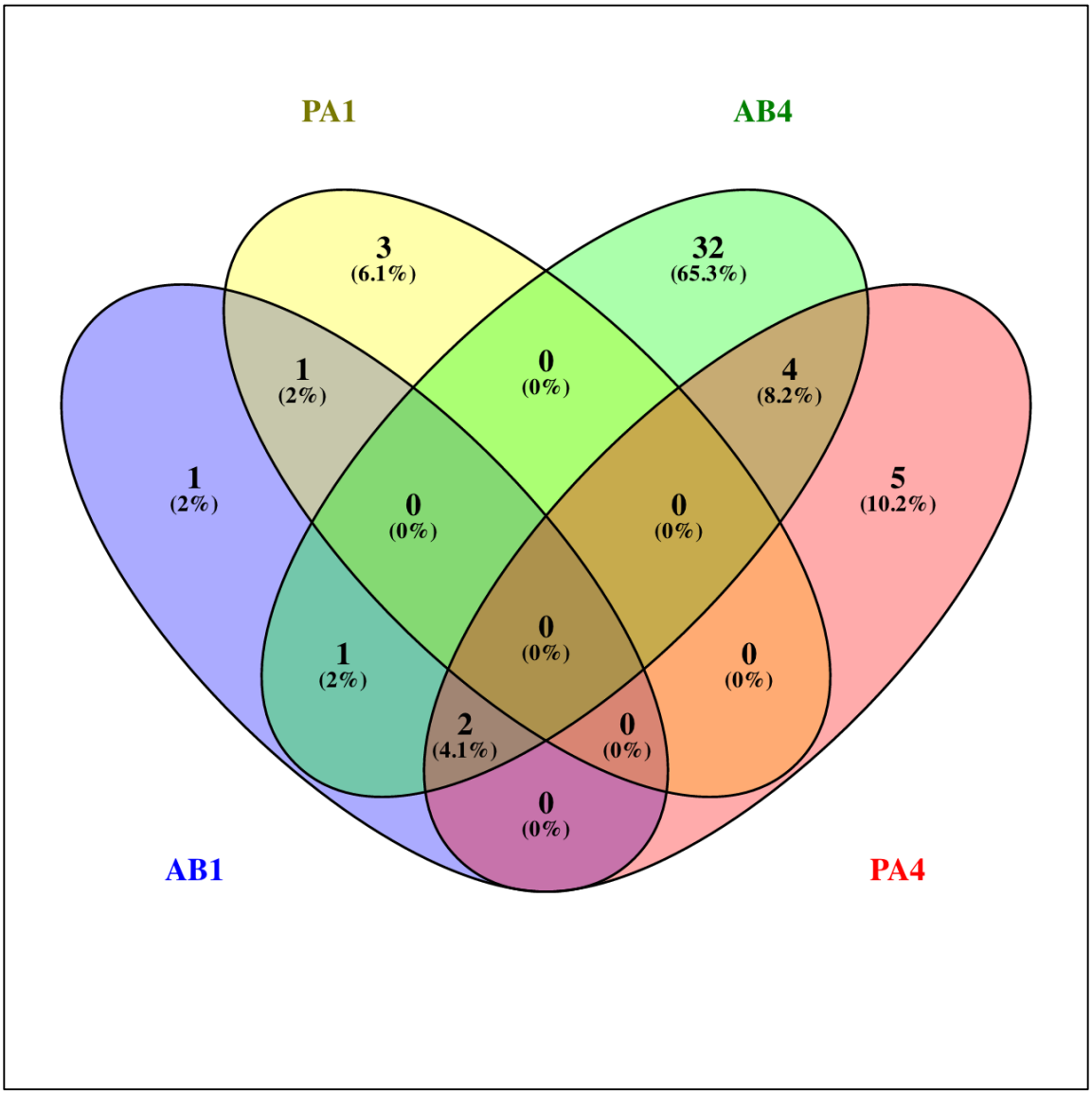

Fig. 16: Four-way Venn diagram displaying overlapping counts of significant differentially expressed genes that are up-regulated.

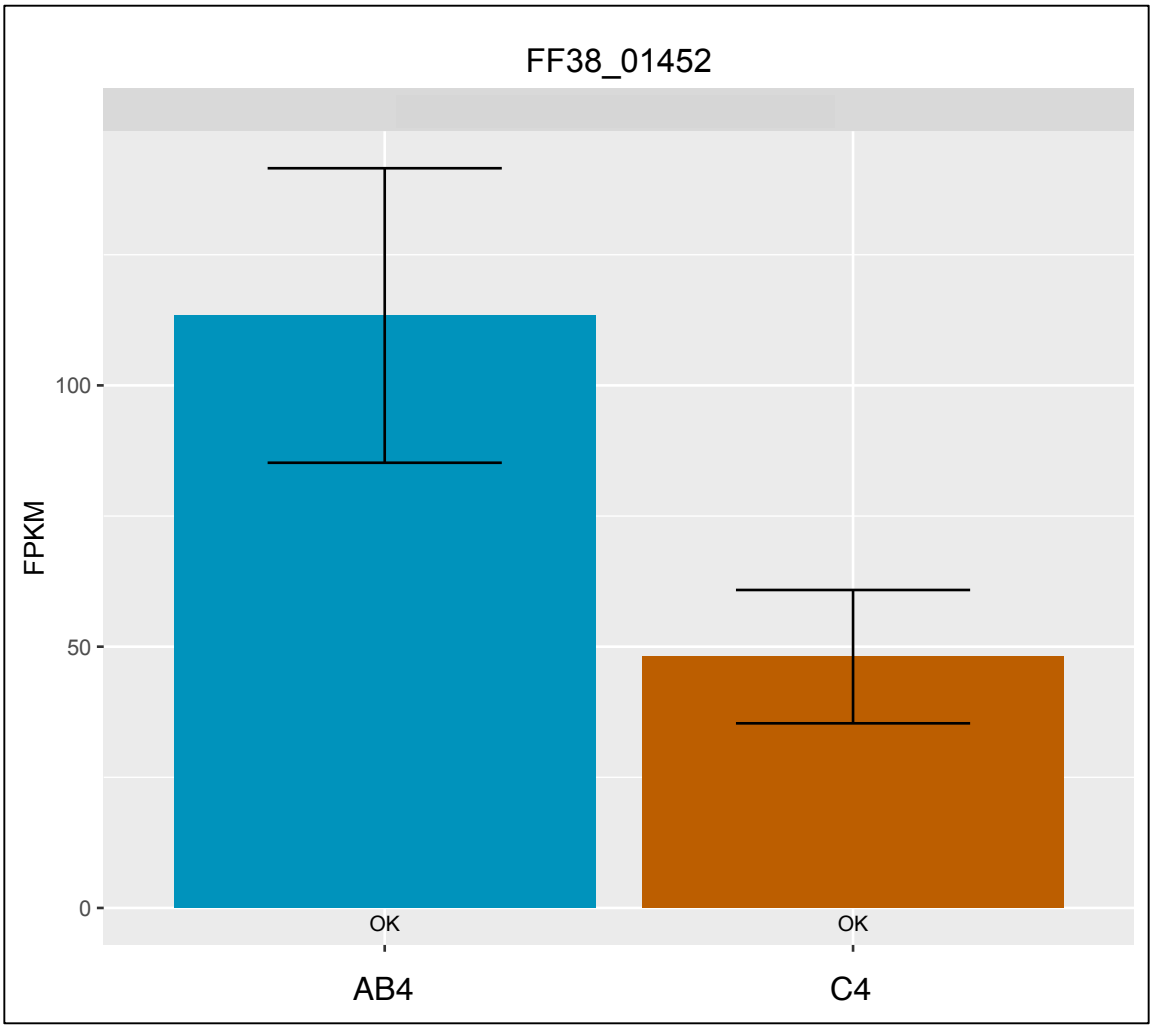

Fig. 17: Barplot displaying expression level fpkm values for gene FF38_01452 (AB4 vs C4). Gene FF38_01452 is associated with a peptidoglycan catabolic process (the chemical reactions and pathways resulting in the breakdown of peptidoglycans, any of a class of glycoconjugates found in bacterial cell walls). FF38_01452 is also up-regulated in PA4 vs C4.

The Panther statistical over-representation test identified up-regulated biological processes that were over-represented in the AB1 vs C1 and the AB4 vs C4 data sets. Four up-regulated genes from the AB1 vs C1 data set had homologous genes in *D. melanogaster*. Three of the four *D. melanogaster* genes mapped to a biological process described as a response to bacterium. The three genes included FF38_09383, FF38_08822, and FF38_04326. There was a 50.06-fold enrichment (P value = 0.0362)

compared to the expected number of genes from this category. Twenty-four up-regulated genes from the AB4 vs C4 data set had homologous genes in *D. melanogaster*. Six of the *D. melanogaster* genes mapped to biological processes described as response to other organism, response to external biotic stimulus, and a response to biotic stimulus. The six genes included FF38_00375, FF38_08822, FF38_01073, FF38_04326, and FF38_08124. There was a 11.65-fold enrichment (P value = 0.0256) compared to the expected number of genes from this category. Genes from the AB4 vs C4 data set that were up-regulated and could be attributed to a known gene in *D. melanogaster* and mapped to a Panther GO-slim Biological process are included in the pie chart in Fig. 18. Up-regulated genes from the AB4 vs C4 data set that could be mapped to a Panther GO-slim molecular function are displayed in Fig. 19. Eight of the 14 categorized genes from the AB4 vs C4 data set mapped to the catalytic activity category.

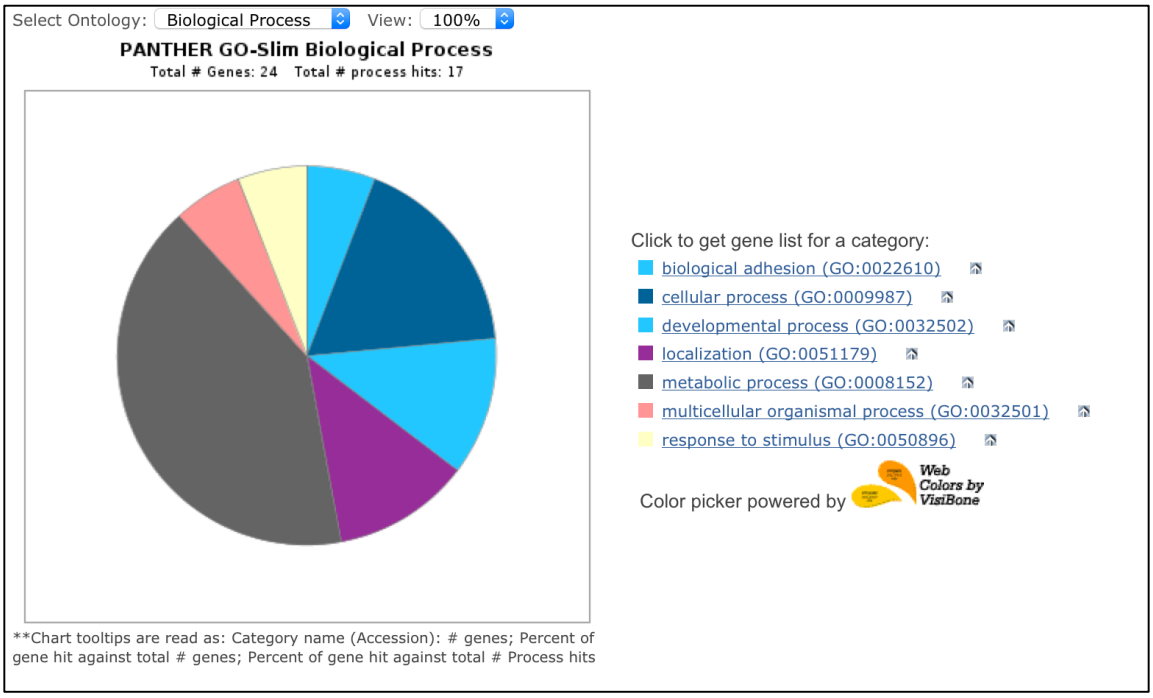

Fig. 18: Panther GO-Slim Biological Process pie chart displaying biological process categories for up-regulated genes from the AB4 vs C4 dataset. Gene ontology analysis was performed only for genes that had homologous genes in *D. melanogaster* that could be mapped to a Panther GO-slim biological process. Calculated using software tools from Mi et al. 2016.

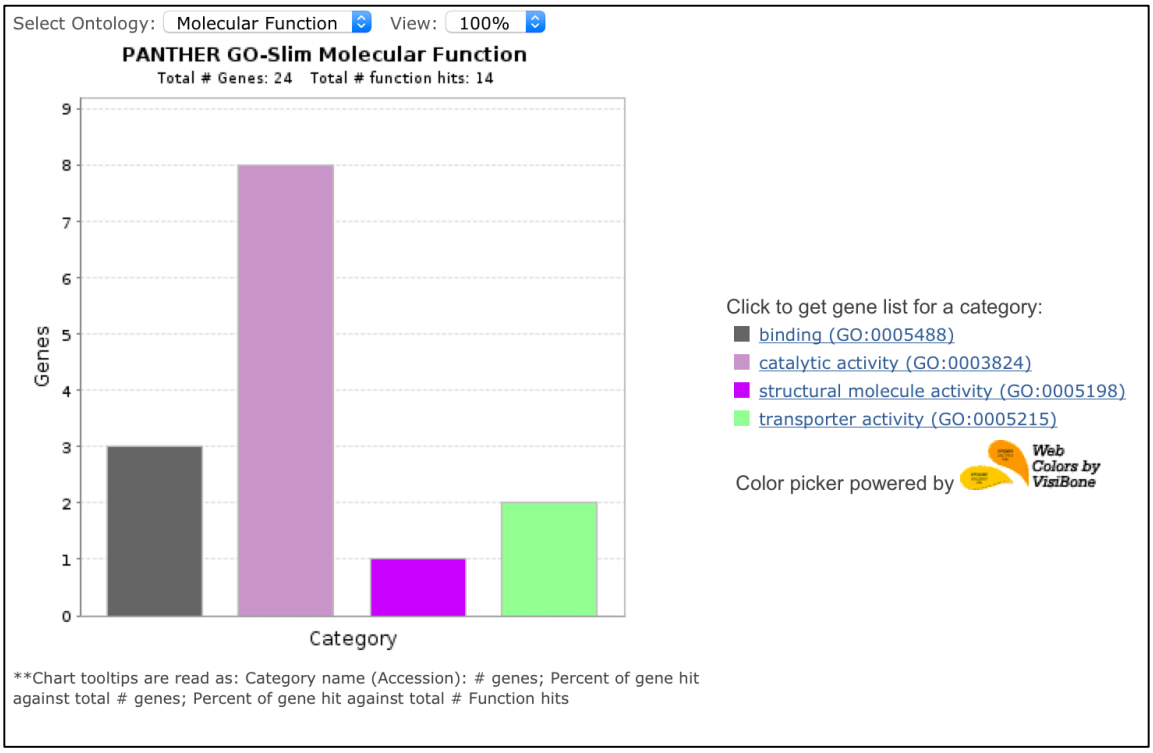

Fig. 19: Panther GO-slim molecular function bar chart displaying molecular function categories for up-regulated genes from the AB4 vs C4 dataset. Gene ontology analysis was performed only for genes that had homologous genes in *D. melanogaster* that could be mapped to a Panther GO-slim molecular function. Calculated using software tools from Mi et al. 2016.

Sequence Alignment to the *L. sericata* Reference Genome

Alignment of one dataset of the RNAseq files to the *L. sericata* genome using the default parameters in TopHat resulted in a concordant pair alignment rate of 48.4%. No further analysis was performed due to the lack of a compatible annotation file at the time of analysis. A summary of the alignment information from the TopHat output is provided in Fig. 20.

```
Sericata genome alignment:
Left reads:
          Input     :  13327997
           Mapped   :   7877023 (59.1% of input)
            of these:    170406 ( 2.2%) have multiple alignments
(223 have >20)
Right reads:
          Input     :  13327997
           Mapped   :   7669743 (57.5% of input)
            of these:    169592 ( 2.2%) have multiple alignments
(223 have >20)
58.3% overall read mapping rate.

Aligned pairs:   6487135
     of these:    145205 ( 2.2%) have multiple alignments
                   42053 ( 0.6%) are discordant alignments
48.4% concordant pair alignment rate.
```

Fig. 20: TopHat output summary of RNAseq alignment to the *L. sericata* reference genome with default parameters.

Discussion

Genes were identified that showed a significant increase or decrease in transcript abundance potentially due to bacterial exposure (Tables 2-9). Identified genes include those associated with antimicrobial activity, immune response, proteolytic activity, catalytic activity, response to gram negative bacteria, and uncharacterized proteins. The ability to assign gene functions or categorize genes that are differentially expressed enables relevant information to be presented. For the genes that were identified and characterized, some were associated with immune responses or antimicrobial activity. Control of Gram-negative bacteria is important in maggot therapy due to the prevalence and severity of wounds infected with antimicrobial resistant Gram-negative bacteria.

In the AB4 vs C4 dataset, six genes were identified that were associated with an over-representation of response to biotic stimulus genes. The predicted functions of these genes include: endopeptidase inhibitor activity- Alpha-2-macroglobulin (Finn et al. 2016), defense response to Gram-negative bacterium in *D. melanogaster* (Attrill et al. 2015), interacting selectively and non-covalently with any protein or protein complex (Finn et al. 2016), establishing a negative feedback loop adjusting Imd pathway activity to the severity of infection in *D. melanogaster* (Attrill et al. 2015), and transferrins-eukaryotic iron-binding glycoproteins that share the common function of controlling the level of free iron in biological fluids (Finn et al. 2016). In the AB1 vs C1 dataset, three genes were identified that were associated with an over-representation of response to bacterium genes. The predicted functions of these genes include: defense response to gram negative bacterium in *D. melanogaster* (Attrill et al. 2015), the antimicrobial peptide Attacin-A (Finn et al. 2016), and establishing a negative feedback loop adjusting Imd pathway activity to the severity of infection in *D. melanogaster* (Attrill et al. 2015). The duration of bacterial exposure (1 h vs 4 h) may explain why more differentially expressed genes were identified in the 4 h data set vs the 1 h dataset. The previously mentioned genes contribute to the insect immune response pathway which includes recognition, signaling, and the transcription of an effector molecule. Some identified genes also play a role in the regulation of these pathways.

In general, there were more changes in transcript abundance when larvae were exposed to bacteria for 4 h vs 1 h. In nutritional studies in *Drosophila,* transcript ratios for some genes were observed to increase in the first hour, accumulate until 7 h, but then

relatively few changes were detected after 7 h (Gershman et al. 2007). For *L. sericata* larvae, bacterial exposure longer than 4 h may lead to the identification of more differentially expressed genes or allow for a greater increase in transcript abundance for some immunity related genes. When Medical Maggots™ are used for medicinal purposes in wound environments, each application of maggots is administered for up to 48 hours (Monarch Labs 2015); RNA-Seq experiments designed with longer bacterial exposure times could correspond more with therapeutic maggot use.

The majority of the differentially expressed genes are unique to a specific time point or bacterial exposure, but some genes are differentially expressed in more than one time point or bacterial exposure (Figs. 5, 6, 14, and 15). For example, gene FF38_01452 shows increased transcript abundance with exposure to *A. baumannii* and *P. aeruginosa* for 4 h. This gene is involved with innate immunity by degrading bacterial peptidoglycans (The UniProt Consortium 2014), a constituent of bacterial cell walls, and so its increased expression level with exposure to different species of bacteria is not surprising.

Significant expression level differences in transcripts due to bacterial exposure were typically low to moderate in terms of $\log_2$ fold change differences. Increased duration of bacterial exposure or increased bacterial load may result in a greater increase in transcript abundance. Although, co-expression of antimicrobial peptides has been observed in Diptera (De Gregorio et al. 2001) and synergism between these peptides would support lower quantities of individual peptides being produced so that a combinatorial effect is more practical and beneficial (Cassone and Otvos Jr 2010, Rolff

and Schmid-Hempel 2016). Specifically, a combination of antimicrobial peptides from *L. sericata* displayed synergistic activity against microbes (Pöppel et al. 2015). Synergistic or combinatorial effects of gene products might explain the observed levels of transcript abundance for relevant genes.

In summary, genes involved with immune response pathways and transcription of antimicrobial peptides are differentially expressed upon larval exposure to Gram-negative bacteria. This study provides insight into the signaling pathways and induced immune responses in *L. sericata*. Further studies could further identify specific proteins or molecules that are produced in response to specific bacteria. In addition, larvae could be genetically engineered or enhanced to be successful against specific bacteria in a wound environment. Information from this study could also provide a framework or supplemental data for studying a similar immune response to pathogens in non-lab strains of *L. sericata* or perhaps in other insects.

CHAPTER III

FUTURE STUDIES AND LIMITATIONS

Antimicrobial peptides that are synthesized during exposure to different species of bacteria could be used as a broad-spectrum therapeutic agent. Further study of the identified transcripts that are unique to a specific type of bacterial exposure could potentially identify gene products that are specific (narrow-spectrum) to a particular bacterial species. Larval exposure to more types of bacteria, including Gram-positive species, could help identify more gene products that are specific to different types of bacteria.

Analyzing the RNA-Seq data with a high quality and well annotated reference genome could improve the sequencing data, and identify, as well as characterize, more genes that are differentially expressed. Future enhancements to software programs or the use of different software programs could potentially enhance the analysis of the RNA-Seq data along expanding the scope of the analysis.

Due to the complex nature of protein synthesis, identifying differentially expressed genes by quantifying increases in transcript abundance does not necessarily mean that those gene products or peptides are being synthesized, secreted or utilized. Also, some identified genes could be incorrectly characterized or misidentified due to technological limitations in the quality of the annotation data. A transcriptomics as well as a proteomics approach would provide a more thorough evaluation of the mechanisms in play. Additional studies could include matching mass spectrometry analysis of the

protein content in larval tissues to identified RNA-Seq data. Also, the antibacterial activity of select peptides can be evaluated by purchasing synthesized peptides and determining the minimum inhibitory concentration (MIC) with exposure to different bacterial species.

Gene products could also be evaluated for the potential to disrupt biofilm formation. Different developmental stages of the larvae could also be incorporated to compare the larval immune response across different developmental stages. Additionally, the larvae could be dissected prior to RNA extraction so that tissue specific RNA could be isolated instead of the whole larval extractions. Tissue specific analysis may yield more functionally relevant information and data has shown that antimicrobial peptides are expressed at higher levels in the fat body as compared to whole larvae (Pöppel et al. 2015). In another study, lucifensin expression was only increased in the fat body with certain infectious environments (Valachova et al. 2013). Genes associated with antimicrobial activity could be expressed at high levels regardless of the larvae being in an infectious environment, but this study was not designed to identify gene expression in this manner. Further data analysis could explore expression levels and sequence information of antimicrobial peptides in the larvae that is not due to bacterial exposure.

REFERENCES

Altschul, S. F., W. Gish, W. Miller, E. W. Myers, and D. J. Lipman. 1990. Basic local alignment search tool. Journal of Molecular Biology 215: 403-410.

Andersen, A. S., B. Joergensen, T. Bjarnsholt, H. Johansen, T. Karlsmark, M. Givskov, and K. A. Krogfelt. 2010a. Quorum-sensing-regulated virulence factors in Pseudomonas aeruginosa are toxic to Lucilia sericata maggots. Microbiology 156: 400-407.

Andersen, A. S., D. Sandvang, K. M. Schnorr, T. Kruse, S. Neve, B. Joergensen, T. Karlsmark, and K. A. Krogfelt. 2010b. A novel approach to the antimicrobial activity of maggot debridement therapy. The Journal of Antimicrobial Chemotherapy 65: 1646-1654.

Anderson, G., and S. L. VanLaerhoven. 1996. Initial studies on insect succession on carrion in southwestern British Columbia. Journal of Forensic Sciences 41: 617-625.

Anderson, G., J. H. Byrd, and J. L. Castner. 2000. Insect succession on carrion and its relationship to determining time of death; Forensic Entomology: The Utility of Arthropods in Legal Investigations 143-175.

Anstead, C. A., P. K. Korhonen, N. D. Young, R. S. Hall, A. R. Jex, S. C. Murali, D. S. T. Hughes, S. F. Lee, T. Perry, A. J. Stroehlein, B. R. E. Ansell, B. Breugelmans, A. Hofmann, J. Qu, S. Dugan, S. L. Lee, H. Chao, H. Dinh, Y. Han, H. V. Doddapaneni, K. C. Worley, D. M. Muzny, P. Ioannidis, R. M. Waterhouse, E. M. Zdobnov, P. J. James, N. H. Bagnall, A. C. Kotze, R. A. Gibbs, S. Richards, P. Batterham, and R. B. Gasser. 2015. Lucilia cuprina genome unlocks parasitic fly biology to underpin future interventions. Nature Communications 6: 7344.

Attrill, H., K. Falls, J. L. Goodman, G. H. Millburn, G. Antonazzo, A. J. Rey, and S. J. Marygold. 2015. FlyBase: establishing a gene group resource for Drosophila melanogaster. Nucleic Acids Research 44: D786-D792.

Baer, W. S. 1931. The treatment of chronic osteomyelitis with the maggot (larva of the blow fly). J Bone Joint Surg Am. 13: 438-475.

Barton, P., S. Cunningham, D. Lindenmayer, and A. Manning. 2013. The role of carrion in maintaining biodiversity and ecological processes in terrestrial ecosystems. Oecologia 171: 761-772.

Beovic, B. 2006. The issue of antimicrobial resistance in human medicine. International Journal of Food Microbiology 112: 280-287.

Bexfield, A., A. E. Bond, E. C. Roberts, E. Dudley, Y. Nigam, S. Thomas, R. P. Newton, and N. A. Ratcliffe. 2008. The antibacterial activity against MRSA strains and other bacteria of a <500Da fraction from maggot excretions/secretions of Lucilia sericata (Diptera: Calliphoridae). Microbes and Infection / Institut Pasteur 10: 325-333.

Birkenhauer, E., S. Neethirajan, and J. S. Weese. 2014. Collagen and hyaluronan at wound sites influence early polymicrobial biofilm adhesive events. BMC Microbiology 14: 191.

Biswal, I., B. S. Arora, D. Kasana, and Neetushree. 2014. Incidence of multidrug resistant pseudomonas aeruginosa isolated from burn patients and environment of teaching institution. Journal of Clinical and Diagnostic Research 8: DC26-29.

Boehme, P., P. Spahn, J. Amendt, and R. Zehner. 2014. The analysis of temporal gene expression to estimate the age of forensically important blow fly pupae: results from three blind studies. International Journal of Legal Medicine 128: 565-573.

Bohova, J., J. Majtan, V. Majtan, and P. Takac. 2014. Selective antibiofilm effects of Lucilia sericata larvae secretions/excretions against wound pathogens. Evidence-based Complementary and Alternative Medicine : eCAM 2014: 857360.

Boucher, H. W., G. H. Talbot, J. S. Bradley, J. E. Edwards, D. Gilbert, L. B. Rice, M. Scheld, B. Spellberg, and J. Bartlett. 2009. Bad bugs, no drugs: No ESKAPE! An update from the Infectious Diseases Society of America. Clinical Infectious Diseases 48: 1-12.

Byrne, A. L., M. A. Camann, T. L. Cyr, E. P. Catts, and K. E. Espelie. 1995. Forensic implications of biochemical differences among geographic populations of the black blow fly, Phormia regina (Meigen). Journal of Forensic Sciences 40: 372-377.

Cassone, M., and L. Otvos Jr. 2010. Synergy among antibacterial peptides and between peptides and small-molecule antibiotics. Expert Review of Anti-infective Therapy 8: 703-716.

Cazander, G., K. E. van Veen, A. T. Bernards, and G. N. Jukema. 2009a. Do maggots have an influence on bacterial growth? A study on the susceptibility of strains of six different bacterial species to maggots of Lucilia sericata and their excretions/secretions. Journal of Tissue Viability 18: 80-87.

Cazander, G., K. E. van Veen, L. H. Bouwman, A. T. Bernards, and G. N. Jukema. 2009b. The influence of maggot excretions on PAO1 biofilm formation on different biomaterials. Clinical Orthopaedics and Related Research 467: 536-545.

Cazander, G., M. C. van de Veerdonk, C. M. Vandenbroucke-Grauls, M. W. Schreurs, and G. N. Jukema. 2010. Maggot excretions inhibit biofilm formation on biomaterials. Clinical Orthopaedics and Related Research 468: 2789-2796.

Cazander, G., D. I. Pritchard, Y. Nigam, W. Jung, and P. H. Nibbering. 2013. Multiple actions of Lucilia sericata larvae in hard-to-heal wounds: larval secretions contain molecules that accelerate wound healing, reduce chronic inflammation and inhibit bacterial infection. BioEssays : News and Reviews in Molecular, Cellular and Developmental Biology 35: 1083-1092.

Cazander, G., M. W. Schreurs, L. Renwarin, C. Dorresteijn, D. Hamann, and G. N. Jukema. 2012. Maggot excretions affect the human complement system. Wound Repair and Regeneration : official publication of the Wound Healing Society [and] the European Tissue Repair Society 20: 879-886.

Centers for Disease Control and Prevention. 2016. 2014 National and State Healthcare-Associated Infections Progress Report. www.cdc.gov/hai/surveillance/progress-report/index.html. Accessed 28 Apr. 2016.

Centers for Disease Control and Prevention. 2017. Antibiotic/antimicrobial resistance. www.cdc.gov/drugresistance/. Accessed 03 Jan. 2017.

Cerovsky, V., J. Zdarek, V. Fucik, L. Monincova, Z. Voburka, and R. Bem. 2010. Lucifensin, the long-sought antimicrobial factor of medicinal maggots of the blowfly Lucilia sericata. Cellular and Molecular Life Sciences : CMLS 67: 455-466.

Chambers, L., S. Woodrow, A. P. Brown, P. D. Harris, D. Phillips, M. Hall, J. C. T. Church, and D. I. Pritchard. 2003. Degradation of extracellular matrix components by defined proteinases from the greenbottle larva Lucilia sericata used for the clinical debridement of non-healing wounds. British Journal of Dermatology 148: 14-23.

Chaudhury, M. F., S. R. Skoda, A. Sagel, and J. B. Welch. 2010. Volatiles emitted from eight wound-isolated bacteria differentially attract gravid screwworms (Diptera: Calliphoridae) to oviposit. J Med Entomol 47: 349-354.

Chopra, I., C. Schofield, M. Everett, A. O'Neill, K. Miller, M. Wilcox, J.-M. Frère, M. Dawson, L. Czaplewski, U. Urleb, and P. Courvalin. 2008. Treatment of health-care-associated infections caused by Gram-negative bacteria: a consensus statement. The Lancet Infectious Diseases 8: 133-139.

Crippen, T. L., and C. Sheffield. 2006. External surface disinfection of the lesser mealworm (Coleoptera: Tenebrionidae). J Med Entomol 43: 916-923.

Daeschlein, G., K. Y. Mumcuoglu, O. Assadian, B. Hoffmeister, and A. Kramer. 2007. In vitro antibacterial activity of Lucilia sericata maggot secretions. Skin pharmacology and physiology 20: 112-115.

Davies, D. G., M. R. Parsek, J. P. Pearson, B. H. Iglewski, J. W. Costerton, and E. P. Greenberg. 1998. The involvement of cell-to-cell signals in the development of a bacterial biofilm. Science 280: 295-298.

De Gregorio, E., P. T. Spellman, G. M. Rubin, and B. Lemaitre. 2001. Genome-wide analysis of the Drosophila immune response by using oligonucleotide microarrays. Proceedings of the National Academy of Sciences 98: 12590-12595.

Deak, D., K. Outterson, J. H. Powers, and A. S. Kesselheim. 2016. Progress in the fight against multidrug-resistant bacteria? a review of u.s. food and drug administration–approved antibiotics, 2010–2015. Annals of Internal Medicine 165: 363-372.

Deron, E. B., J. D. Parker, C. B. Woodson, H. J. Mills, J. Kubanek, P. A. Sobecky, and M. E. Hay. 2006. Chemically mediated competition between microbes and animals: microbes as consumers in food webs. Ecology 87: 2821-2831.

Diaz-Roa, A., M. A. Gaona, N. A. Segura, D. Suarez, M. A. Patarroyo, and F. J. Bello. 2014. Sarconesiopsis magellanica (Diptera: Calliphoridae) excretions and secretions have potent antibacterial activity. Acta Tropica 136: 37-43.

Doshi, P. 2015. Speeding new antibiotics to market: a fake fix? BMJ : British Medical Journal 350: h1453.

Finn, R. D., T. K. Attwood, P. C. Babbitt, A. Bateman, P. Bork, A. J. Bridge, H.-Y. Chang, Z. Dosztányi, S. El-Gebali, M. Fraser, J. Gough, D. Haft, G. L. Holliday, H. Huang, X. Huang, I. Letunic, R. Lopez, S. Lu, A. Marchler-Bauer, H. Mi, J. Mistry, D. A. Natale, M. Necci, G. Nuka, C. A. Orengo, Y.

Park, S. Pesseat, D. Piovesan, S. C. Potter, N. D. Rawlings, N. Redaschi, L. Richardson, C. Rivoire, A. Sangrador-Vegas, C. Sigrist, I. Sillitoe, B. Smithers, S. Squizzato, G. Sutton, N. Thanki, P. D. Thomas, Silvio C. E. Tosatto, C. H. Wu, I. Xenarios, L.-S. Yeh, S.-Y. Young, and A. L. Mitchell. 2016. InterPro in 2017—beyond protein family and domain annotations. Nucleic Acids Research 45: D190-D199.

Frederickx, C., J. Dekeirsschieter, F. J. Verheggen, and E. Haubruge. 2012. Responses of Lucilia sericata Meigen (Diptera: Calliphoridae) to cadaveric volatile organic compounds. Journal of Forensic Sciences 57: 386-390.

Gelbart, W. M., and D. B. Emmert. 2010. FlyBase high throughput expression pattern data beta version. flybase.org. Accessed 23 Mar. 2015.

Gentleman, R. C., V. J. Carey, D. M. Bates, B. Bolstad, M. Dettling, S. Dudoit, B. Ellis, L. Gautier, Y. Ge, J. Gentry, K. Hornik, T. Hothorn, W. Huber, S. Iacus, R. Irizarry, F. Leisch, C. Li, M. Maechler, A. J. Rossini, G. Sawitzki, C. Smith, G. Smyth, L. Tierney, J. Y. Yang, and J. Zhang. 2004. Bioconductor: open software development for computational biology and bioinformatics. Genome Biol 5: R80.

Gershman, B., O. Puig, L. Hang, R. M. Peitzsch, M. Tatar, and R. S. Garofalo. 2007. High-resolution dynamics of the transcriptional response to nutrition in drosophila: a key role for dFOXO. Physiological Genomics 29: 24.

Goldstein, H. I. 1931. Maggots in the treatment of wounds, compound fractures and osteomyelitis. JAMA: The Journal of the American Medical Association 96: 290.

Harrison, P. F., and J. Lederberg. 1998. Antimicrobial resistance : issues and options: workshop report, National Academy Press, Washington, D.C.

Janzen, D. H. 1977. Why fruits rot, seeds mold, and meat spoils. The American Naturalist 111: 691-713.

Johnson, E. N., T. C. Burns, R. A. Hayda, D. R. Hospenthal, and C. K. Murray. 2007. Infectious complications of open type III tibial fractures among combat casualties. Clinical Infectious Diseases 45: 409-415.

Kersey, P. J., J. E. Allen, I. Armean, S. Boddu, B. J. Bolt, D. Carvalho-Silva, M. Christensen, P. Davis, L. J. Falin, C. Grabmueller, J. Humphrey, A. Kerhornou, J. Khobova, N. K. Aranganathan, N. Langridge, E. Lowy, M. D. McDowall, U. Maheswari, M. Nuhn, C. K. Ong, B. Overduin, M. Paulini, H. Pedro, E. Perry, G. Spudich, E. Tapanari, B. Walts, G. Williams, M. Tello–Ruiz, J. Stein, S. Wei, D. Ware, D. M. Bolser, K. L. Howe, E. Kulesha, D.

Lawson, G. Maslen, and D. M. Staines. 2016. Ensembl Genomes 2016: more genomes, more complexity. Nucleic Acids Research 44: D574-D580.

Kinsella, R. J., A. Kähäri, S. Haider, J. Zamora, G. Proctor, G. Spudich, J. Almeida-King, D. Staines, P. Derwent, A. Kerhornou, P. Kersey, and P. Flicek. 2011. Ensembl BioMarts: a hub for data retrieval across taxonomic space. Database: The Journal of Biological Databases and Curation 2011: bar030.

Lawrence, R., and E. Jeyakumar. 2013. Antimicrobial resistance: a cause for global concern. BMC Proceedings 7: S1.

Liu, W., M. Longnecker, A. M. Tarone, and J. K. Tomberlin. 2016. Responses of Lucilia sericata (Diptera: Calliphoridae) to compounds from microbial decomposition of larval resources. Animal Behaviour 115: 217-225.

Livermore, D. M. 2003. Bacterial resistance- Origins, epidemiology, and impact. Clinical Infectious Diseases: S11-23.

Love, M. I., W. Huber, and S. Anders. 2014. Moderated estimation of fold change and dispersion for RNA-seq data with DESeq2. Genome Biology 15: 1-21.

Ma, Q., A. Fonseca, W. Liu, A. T. Fields, M. L. Pimsler, A. F. Spindola, A. M. Tarone, T. L. Crippen, J. K. Tomberlin, and T. K. Wood. 2012. Proteus mirabilis interkingdom swarming signals attract blow flies. ISME J 6: 1356-1366.

Maragakis, L. L., and T. M. Perl. 2008. Acinetobacter baumannii: epidemiology, antimicrobial resistance, and treatment options. Clinical Infectious Diseases : an official publication of the Infectious Diseases Society of America 46: 1254-1263.

Mi, H., S. Poudel, A. Muruganujan, J. T. Casagrande, and P. D. Thomas. 2016. PANTHER version 10: expanded protein families and functions, and analysis tools. Nucleic Acids Research 44: D336-D342.

Mihu, M. R., and L. R. Martinez. 2011. Novel therapies for treatment of multi-drug resistant Acinetobacter baumannii skin infections. Virulence 2: 97-102.

Monarch Labs. 2015. Medical MaggotsTM. Product insert Rev_D.

Mumcuoglu, K. Y., J. Miller, M. Mumcuoglu, M. Friger, and M. Tarshis. 2001. Destruction of bacteria in the digestive tract of the maggot of Lucilia sericata (Diptera: Calliphoridae). Journal of Medical Entomology 38: 161-166.

Mumcuoglu, K. Y., A. Ingber, L. Gilead, J. Stessman, R. Friedmann, H. Schulman, H. Bichucher, I. Ioffe-Uspensky, J. Miller, R. Galun, and I. Raz. 1998. Maggot therapy for the treatment of diabetic foot ulcers. Diabetes Care 21: 2030-2031.

Newswire, P. R. 2016. Antibiotics: Technologies and global markets, LON-Reportbuyer. Y.

Nigam, Y., A. Bexfield, S. Thomas, and N. A. Ratcliffe. 2006. Maggot therapy: The science and implication for CAM Part I—History and bacterial resistance. Evidence-based Complementary and Alternative Medicine 3: 223-227.

O'Neill, J. 2016. Tackling drug-resistant infections globally: final report and recommendations. Government of the United Kingdom.

O'Shea, M. K. 2012. Acinetobacter in modern warfare. International Journal of Antimicrobial Agents 39: 363-375.

Oliveros, J. C. 2007-2015. Venny. An interactive tool for comparing lists with Venn's diagrams. www.bioinfogp.cnb.csic.es/tools/venny/index.html. Accessed 15 Jan. 2017.

Parmenter, R. R., and J. A. MacMahon. 2009. Carrion decomposition and nutrient cycling in a semiarid shrub—steppe ecosystem. Ecological Monographs 79: 637-661.

Peleg, A. Y., H. Seifert, and D. L. Paterson. 2008. Acinetobacter baumannii: emergence of a successful pathogen. Clinical microbiology reviews 21: 538-582.

Pöppel, A.-K., H. Vogel, J. Wiesner, and A. Vilcinskas. 2015. Antimicrobial peptides expressed in medicinal maggots of the blow fly Lucilia sericata show combinatorial activity against bacteria. Antimicrobial Agents and Chemotherapy 59: 2508-2514.

R Core Team 2016. R: A language and environment for statistical computing computer program, version By R Core Team, Vienna, Austria. www.r-project.org. Accessed 30 Nov. 2016.

Rolff, J., and P. Schmid-Hempel. 2016. Perspectives on the evolutionary ecology of arthropod antimicrobial peptides. Philosophical Transactions of the Royal Society B: Biological Sciences 371: 1695.

Rozen, D. E., D. J. P. Engelmoer, and P. T. Smiseth. 2008. Antimicrobial strategies in burying beetles breeding on carrion. Proceedings of the National Academy of Sciences of the United States of America 105: 17890-17895.

ScienceNews. 1931. Science news. Science 74: 10a-13a.

Shendure, J., and H. Ji. 2008. Next-generation DNA sequencing. Nat Biotech 26: 1135-1145.

Sherman, R. A. 2002. Maggot therapy for foot and leg wounds. The International Journal of Lower Extremity Wounds 1: 135-142.

Sherman, R. A. 2014. Mechanisms of maggot-induced wound healing: what do we know, and where do we go from here? Evidence-based Complementary and Alternative Medicine : eCAM 2014: 592419.

Sherman, R. A., M. J. R. Hall, and S. Thomas. 2000. Medicinal maggots: an ancient remedy for some contemporary afflictions. Annual Review of Entomology 45: 55-81.

Statheropoulos, M., C. Spiliopoulou, and A. Agapiou. 2005. A study of volatile organic compounds evolved from the decaying human body. Forensic Science International 153: 147-155.

Sze, S. H., J. P. Dunham, B. Carey, P. L. Chang, F. Li, R. M. Edman, C. Fjeldsted, M. J. Scott, S. V. Nuzhdin, and A. M. Tarone. 2012. A de novo transcriptome assembly of Lucilia sericata (Diptera: Calliphoridae) with predicted alternative splices, single nucleotide polymorphisms and transcript expression estimates. Insect Molecular Biology 21: 205-221.

Talbot, G. H., J. Bradley, J. E. Edwards, D. Gilbert, M. Scheld, and J. G. Bartlett. 2006. Bad bugs need drugs: an update on the development pipeline from the antimicrobial availability task force of the Infectious Diseases Society of America. Clinical Infectious Diseases 42: 657-668.

Tarone, A. M., and D. R. Foran. 2011. Gene expression during blow fly development: improving the precision of age estimates in forensic entomology. Journal of Forensic Sciences 56 Suppl 1: S112-122.

Teh, C. H., W. A. Nazni, H. L. Lee, A. Fairuz, S. B. Tan, and M. Sofian-Azirun. 2013. In vitro antibacterial activity and physicochemical properties of a crude methanol extract of the larvae of the blow fly Lucilia cuprina. Medical and Veterinary Entomology 27: 414-420.

The UniProt Consortium. 2014. UniProt: a hub for protein information. Nucleic Acids Research 43: D204-D212.

Thomas, P. D., A. Kejariwal, N. Guo, H. Mi, M. J. Campbell, A. Muruganujan, and B. Lazareva-Ulitsky. 2006. Applications for protein sequence–function evolution data: mRNA/protein expression analysis and coding SNP scoring tools. Nucleic Acids Research 34: W645-W650.

Tomberlin, J. K., T. L. Crippen, A. M. Tarone, B. Singh, K. Adams, Y. H. Rezenom, M. E. Benbow, M. Flores, M. Longnecker, J. L. Pechal, D. H. Russell, R. C. Beier, and T. K. Wood. 2012. Interkingdom responses of flies to bacteria mediated by fly physiology and bacterial quorum sensing. Animal Behaviour 84: 1449-1456.

Trapnell, C., L. Pachter, and S. L. Salzberg. 2009. TopHat: discovering splice junctions with RNA-Seq. Bioinformatics (Oxford, England) 25: 1105-1111.

Trapnell, C., B. A. Williams, G. Pertea, A. Mortazavi, G. Kwan, M. J. van Baren, S. L. Salzberg, B. J. Wold, and L. Pachter. 2010. Transcript assembly and quantification by RNA-Seq reveals unannotated transcripts and isoform switching during cell differentiation. Nat Biotech 28: 511-515.

Trapnell, C., A. Roberts, L. Goff, G. Pertea, D. Kim, D. R. Kelley, H. Pimentel, S. L. Salzberg, J. L. Rinn, and L. Pachter. 2012. Differential gene and transcript expression analysis of RNA-seq experiments with TopHat and Cufflinks. Nature Protocols 7: 562-578.

Valachova, I., J. Bohova, Z. Palosova, P. Takac, M. Kozanek, and J. Majtan. 2013. Expression of lucifensin in Lucilia sericata medicinal maggots in infected environments. Cell and Tissue Research 353: 165-171.

Valachova, I., E. Prochazka, J. Bohova, P. Novak, P. Takac, and J. Majtan. 2014. Antibacterial properties of lucifensin in Lucilia sericata maggots after septic injury. Asian Pacific Journal of Tropical Biomedicine 4(5): 358-361.

van der Plas, M. J. A., M. Baldry, J. T. van Dissel, G. N. Jukema, and P. H. Nibbering. 2009. Maggot secretions suppress pro-inflammatory responses of human monocytes through elevation of cyclic AMP. Diabetologia 52: 1962-1970.

Vilcinskas, A. 2013. Evolutionary plasticity of insect immunity. Journal of Insect Physiology 59: 123-129.

Wilson, S. J., C. J. Knipe, M. J. Zieger, K. M. Gabehart, J. E. Goodman, H. M. Volk, and R. Sood. 2004. Direct costs of multidrug-resistant Acinetobacter baumannii in the burn unit of a public teaching hospital. American Journal of Infection Control 32: 342-344.

Wise, R., T. Hart, O. Cars, M. Streulens, R. Helmuth, P. Huovinen, and M. Sprenger. 1998. Antimicrobial resistance. Is a major threat to public health. BMJ (Clinical Research Ed.) 317: 609-610.